

*Sliding wear behaviour of zircon sand reinforced LM13 alloy  
prepared by spray forming technique*

*Thesis submitted in partial fulfilment of the requirement for  
The award of the degree of*

**Master of Technology (M. Tech.)**

In

**MATERIALS AND METALLURGICAL ENGINEERING**

Submitted by

**RASHMI MITTAL**

**Roll No. : 600802019**

Under the guidance of

**Dr. O.P PANDEY**

Head of the Department

School of Physics & Materials Science



School of Physics & Materials Science

Thapar University, Patiala

**July 2010**

## CERTIFICATE

I hereby certify that the work which is being presented in the thesis entitled, "*Sliding wear behavior of zircon sand reinforced LM13 alloy prepared by spray forming technique*" submitted by Ms. RASHMI MITTAL, Roll No. 600802019 in the partial fulfillment of the requirements for the award of degree of **MASTERS OF TECHNOLOGY** in "**Materials and Metallurgical Engineering**" from the **School of Physics and Material Science of Thapar University, Patiala**, is an authentic record of my own work carried out under the supervision of Dr. O.P. Pandey and refers other researcher's work which are duly listed in the reference section.

This is to certify that the above statement made by the candidate is correct and true to the best of my knowledge.

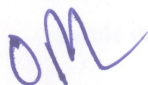


(Prof. O.P. Pandey)

Supervisor

Thapar University, Patiala-147001

Countersigned by:



Dr. O.P. Pandey,  
Professor and Head of the Department,  
Thapar University,  
Patiala, Punjab.

  
21.2.16

Dr. R.K. Sharma  
Dean Academic Affairs,  
Thapar University,  
Patiala, Punjab.

## **ACKNOWLEDGEMENT**

At this momentous occasion of binding my thesis I would like to acknowledge the contribution of all those benevolent people. I have been blessed to associate with. Behind every student, there stand a myriad of people whose help and contribution makes things successful. Since such a list can be a prohibitively long, we may be excused for any omissions. My first and foremost offering of thanks goes to the architect who shaped my dreams into reality, my guide and mentor **Dr. O.P. Pandey, Professor and Head, School of Physics and Materials Science.**

I also thanks to **Miss. Kamalpreet Kaur (Research Scholar)** for her guidance in whole project work without whom this project work can not be completed.

My greatest thanks are to **Dr. Kulvir Singh, Associate Professor and PG Incharge, School of Physics and Materials Science** for his encouragement and execution of thesis work. I would also like to thank **Dr. K.K. Raina, Professor and Deputy Director, School Of Physics and Materials Science** for his guidance and encouragement. I am also thankful to **Dr. D.P. Singh, Dr. Puneet Sharma, Dr. S.D. Tiwari** and all the faculty members of School of Physics and Materials Science for their constructive suggestions at different stages of this work.

My special thanks to Lab supdt.(SPMS), **Mr. Purshottam.** His assistance and partnership were of great pleasure. His comments and views were very insightful and helpful.

I would also like to thank **Mr. Jant Singh** for providing all kind of assistance in PG Lab for creating a healthy research environment.

I would like to convey my sincere gratitude to my friends and colleagues **Ramkishor, Gaurav Singla, Rajni, Paramjot, Poonam Sharma, Poonam Benjwal,** for their support and their timely help and valuable discussions.

I owe my sincere thanks to all the staff members of School of Physics and Materials Science for their support and encouragement. The meaning of my life and work is incomplete without paying regards to my respected parents whose blessings and continuous encouragement have shown me the path to achieve my goals. And above all, I pay my regards to the **Almighty** for his love and blessings.

*(Rashmi Mittal)*

## **ABSTRACT**

In present work, we have studied the wear behavior of LM13 alloy and LM13/zircon sand composite prepared by spray forming technique. For the comparative purpose the spray formed LM13 alloy is tested under dry sliding condition at different temperature. The wear rate of spray formed composite is significantly lower than the as cast LM13 alloy. The microstructure of spray formed composite is characterized by fine size equiaxed grain. The reinforced particles are equally distributed throughout the matrix of the composite. The as prepared samples were studied using SEM and X-ray diffraction techniques. The XRD results indicate the different phases present in the matrix. Hardness of the prepared samples also has been tested. Mode of wear mechanism has been analyzed from SEM micrograph of worn pin surface and collected debris during the dry sliding run. Composites are found to offer greater wear resistance than base alloy.

# CONTENTS

---

## LIST OF FIGURES

## LIST OF TABLES

<b>CHAPTER 1 INTRODUCTION</b>		<b>PAGE No.</b>
1.1	Metal matrix composite	(1)
1.2	Aluminium metal matrix composite	(2)
1.3	Zircon sand as reinforcement	(3)
1.3.1	Advantages of using zircon sand as reinforcement	(3)
1.4	Processing techniques	(3)
1.5	Objective	(5)
<b>CHAPTER-2 PROCESSING TECHNIQUES</b>		
2.1	History of spray casting	(8)
2.2	Atomization	(9)
2.2.1	Centrifugal atomization	(9)
2.2.2	Gas atomization	(11)
2.3	Mechanisms of atomization	(14)
2.4	Deposition and preform solidification	(16)
2.5	Metallurgical characteristics of spray formed alloys	(17)
2.6	Spray formed microstructure	(17)

2.7	Application	(19)
2.8	Advantages	(19)
2.9	Disadvantages	(20)
2.10	Commercialization	(21)
	<b>CHAPTER-3 LITERATURE REVIEW</b>	<b>(23)</b>
	<b>CHAPTER-4 EXPERIMENTAL WORK</b>	<b>(30)</b>
	<b>CHAPTER-5 RESULTS AND DISCUSSION</b>	<b>(34)</b>
	<b>CHAPTER-6 CONCLUSION AND FUTURE SCOPE</b>	<b>(50)</b>
	<b>REFERENCES</b>	<b>(52)</b>

## LIST OF FIGURES

---

**Fig.2.1** Mode of addition of particles (a) through dispenser, (b) premixing in the crucible.

**Fig.2.2** Systematic representation of centrifugal atomization.

**Fig.2.3** Schematic of (a) free fall or open atomizer, and (b) a closed coupled or closed atomizer.

**Fig.2.4** Schematic of (a) an annular atomizer, (b) a multi jet atomizer and (c) a linear atomizer.

**Fig.2.5** Schematic of (a) pneumatic and (b) mechanical scanning atomizer arrangement.

**Fig.2.6** Typical polygonal as spray formed Ni superalloy billets.

**Fig.3.1** Al-Si (hypereutectic alloy).

**Fig. 4.1:** Spray casting set up.

**Fig.5.1** XRD pattern of LM13 alloy and spray formed composites.

**Fig.5.2** Microstructure of (a) cast LM13 alloy, (b) spray cast LM13 alloy, (c) LM13-5Sn/zircon sand (63), (d) LM13-5Sn/zircon sand (106), (e) LM13-10Sn/zircon sand (106).

**Fig.5.3** Rockwell hardness of different compositions.

**Fig.5.4.1** Variation of wear rate vs. sliding distance for cast LM13 alloy at (a) 50°C (b) 75°C.

**Fig.5.4.2** Variation of wear rate vs. sliding distance for spray formed LM13 alloy at (a) 50°C (b) 75°C.

**Fig.5.4.3** Variation of wear rate vs. sliding distance for  $ZrSiO_4(63)$  reinforced LM13-5Sn at (a) 50°C (b) 75°C.

**Fig.5.4.4** Variation of wear rate vs. sliding distance for  $ZrSiO_4(106)$  reinforced LM13-5Sn at(a) 50°C (b) 75°C

**Fig.5.4.5** Variation of wear rate vs. sliding distance for  $ZrSiO_4(106)$  reinforced LM13-10Sn at (a) 50°C (b) 75°C.

**Fig.5.4** Average wear rate of materials (1-cast LM13; 2-spray formed LM13; 3-LM13-5Sn/zircon sand(106); 4- LM13-5Sn/ zircon sand(63); 5- LM13-10Sn/zircon sand(106) at 50°C and 75°C for (a)2.5 kg, (b)3.5kg and (c)4.5kg load.

**Fig.5.5** At 3.5 kg load SEM images of (a) worn surface of cast LM13 at 75°C, (b) debris of cast LM13 at 75°C, (c) worn surface of spray cast LM13 at 75°C, (d) debris of spray cast LM13 at 75°C, (e) worn surface of LM13-10Sn/zircon sand<sub>106</sub> at 50°C, (f) debris of LM13-10Sn/zircon sand<sub>106</sub> at 50°C, (g) worn surface of LM13-10Sn/zircon sand<sub>106</sub> at 75°C, (h) debris of LM13-10Sn/zircon sand<sub>106</sub> at 75°C.

## LIST OF TABLES

---

**Table 1** Reduction of process steps for spray formed preforms in comparison with powder metallurgy.

**Table 2** A comparison of single and twin atomizers for spray deposition of high speed steel billets.

**Table 3** Relationship between spray conditions, perform condition and deposition behaviour during spray forming.

**Table 4.1** Chemical composition of LM13 alloy.

**Table 4.2** Particle size range of zircon sand.

**Table 4.3** Chemical composition of zircon sand.

**Table 4.4** Chemical composition of Keller' reagent.

.

# CHAPTER-1

## INTRODUCTION

---

The particulate reinforced composites have been considered to provide an attractive alternative to the traditional un-reinforced monolithic alloys. The reinforcement material is embedded into the matrix. The reinforcement does not always serve a purely structural task, but is also used to change physical properties such as wear resistance, friction coefficient or thermal conductivity. For example, SiC particle introduced into the metal matrix is beneficial for mechanical strength. Zircon reinforced composite shows better wear resistance than alumina reinforced composite due to its superior particle-matrix bonding [1].

### 1.1 Metal matrix composite (MMC)

The matrix is the monolithic material into which the reinforcement is embedded and is completely continuous. This means that there is a path through the matrix to any point in the material, unlike two materials sandwiched together. In structural applications, the matrix is usually a lighter metal such as aluminium, magnesium or titanium, and provides a compliant support for the reinforcement.

A metal matrix composite (MMC) is composite material with at least two constituent parts, one being a metal. The other material may be a different metal or another material such as a ceramic or organic compound. When at least three materials are present, it is called a hybrid composite.

MMCs are made by dispersing a reinforcing material into a metal matrix. The reinforcement surface can be coated to prevent a chemical reaction with the matrix. For example, carbon fibers are commonly used in aluminium matrix to synthesize composites containing low density and high strength. However, carbon reacts with aluminium to generate a brittle and water-soluble compound  $Al_4C_3$  on the surface of the fiber. To prevent this reaction, the carbon fibers are coated with nickel or titanium boride.

MMCs are of two types.

- (1) Discontinuous MMCs
- (2) Continuous MMCs

Discontinuous MMCs can be isotropic and can be worked with standard metal working techniques such as extrusion, forging or rolling. In addition they may be machined using conventional techniques, but commonly would need the use of polycrystalline diamond tooling. Continuous reinforcement uses monofilament wires or fibers such as carbon fiber or silicon carbide because the fibers are embedded into the matrix in a certain direction. The result is an anisotropic structure in which the alignment of the material affects its strength. One of the first MMCs used boron filament as reinforcement. Discontinuous reinforcement uses "Whiskers", short fibers and particles. The most common reinforcing materials in this category are alumina and silicon carbide. A large number of composite materials have metallic matrices reinforced with high strength, high modulus and often brittle ceramic phase particles. A uniform dispersion of reinforcement materials in the metal matrix offers improvement in strength, elastic modulus, corrosion and wear resistance of resultant composites. Due to these properties, a particulate reinforced composite finds a wide range of applications in automotive and aerospace industries compared to their counterpart monolithic alloys.

## **1.2 Aluminium metal matrix composite**

Aluminium based metal matrix composites (AMCs) are promising materials for automotive, aerospace, deep ocean, nuclear energy generation and other structural applications because of their low density, high stiffness and low wear rate. Discontinuously reinforced AMCs containing particulates are of particular interest to industrial community owing to their isotropic behavior. AMCs are prepared using both solid state route (blending, compacting and sintering of powders) and liquid state route, such as infiltration, stir casting, squeeze casting and spray forming, etc. Each of these processes has their own merit and limitations. Out of these, spray forming method has drawn significant interest owing to its ability to form near-net shape product in one single step. The spray forming process results in unique microstructure consisting of fine equiaxed grains with reduced macro and micro segregation [2]. The rapid solidification helps to reduce the interfacial degradation due to in situ reaction between particles and matrix. In addition, it offers several advantages arising from rapid solidification, such as grain refinement, extension of solid solubility limit, homogeneous microstructure etc.

Properties of Al-MMC's are

- a) High thermal conductivity
- b) Low thermal expansion
- c) Low relative density as compared to cast iron

### **1.3 Zircon sand as reinforcement**

Zircon sand consists of mostly zirconium silicate ( $ZrSiO_4$ ) and some rare earth elements, titanium minerals, monazite, etc. Zircon is used chiefly for facing on foundry moulds to increase the resistance against metal penetration. Zircon was found to be a promising candidate as reinforcement material for aluminium, zinc and lead based composites.

#### **1.3.1 Advantages of using zircon sand as reinforcement**

Zircon possesses a very low thermal expansion coefficient compared to most other ceramic oxides. Therefore a change in temperature would not give rise to very high thermal stresses within zircon particles. Zircon reinforced composite shows better wear resistance than alumina reinforced composite due to its superior particle-matrix bonding. There are many advantages of using zircon sand as reinforcement:

1. High hardness,
2. High modulus of elasticity,
3. High temperature resistance,
4. Acid corrosion resistance and excellent thermal stability[1]

### **1.4 Processing techniques**

There are several reviews available on processing, properties and interfacial phenomenon in composites. Currently, techniques are available for processing of composite materials. Liquid metallurgy (LM) or powder metallurgy (PM) routes are used in industries for large scale production. In the former, the particulate phases are mechanically dispersed in the liquid before solidification of the melt. Whereas in the latter, either elemental or pre-alloyed powders are blended with particulates and compacted by hot pressing and hot extrusion processes. Relatively low solid-liquid interface velocity associated with slow cooling rate of the melt and poor wettability of the melt with the second phase particles generate non-uniform distribution of

second phase particles in the matrix phase. In addition slow cooling rate of the melt provides dendritic solidification structure of the cast composites. Consequently, secondary processing methods are adopted to achieve their microstructural refinement as well as chemical homogeneity. A high degree of melt superheat often used in the liquid metallurgy method results in reaction interfaces between the matrix and particulates. This effect deteriorates mechanical properties of composites. Alternatively, the reaction interfaces are although significantly reduced in powder metallurgy processing route, this processing methodology requires expensive equipments in powder consolidation by hot extrusion or hot-isotatic pressing. In addition, different processing methods also results in a composite material having properties that are different from each other.

Several shortcomings of conventional LM and PM methods of synthesizing composite materials are overcome in spray forming. In this processing technique, high energy gas jets interact with the stream of metallic melt to generate a spray of micron size droplets. These are subsequently deposited on a stationary or movable substrates to achieve a near-net shape perform. The reinforcement particles are injected in the spray of droplets at a suitable distance from the atomizer which are simultaneously deposited on the substrate to generate a preform of the composite material. A high heat extraction rate achievable during solidification of droplets as well as on the deposition surface provides several beneficial effects to the composites produced by this technique.

Rapid solidification inherent in spray deposition generates a considerable refinement in the grain size with equiaxed grain morphology and chemical homogeneity of the matrix phase. Incorporation of small volume fraction of a reactive gas in the atomization chamber results in formation of oxide particles finely dispersed in the matrix phase [3].

**Table 1** Reduction of process steps for spray formed preforms in comparison with powder metallurgy [4].

<b>Conventional Process</b>	<b>Powder Metallurgy</b>	<b>Spray Forming</b>
Melt	Melt	Melt
Cast	Atomize	Spray form
Heat	Sieve	Crop ends
Pre-roll	Make capsule	
Grind	Fill capsule	
Anneal	Seal capsule	Anneal
Forge	Cold isostatic press	
Crop ends		
Cut		
Peel turn		Peel turn
Bore		
Expand		
Extrude	Extrude	
Crop ends	Crop ends	
Pickle	Remove capsule	
Cold pilger	Cold pilger	Cold pilger

## 1.5 Objective

The increasing demand from many industries for improved properties in materials has stimulated the development of new materials. For the automotive industry, the properties most required are reduced weight, low thermal expansion coefficient and excellent mechanical properties; mainly wear resistance at high temperatures. In this context, various new materials such as the Al-Si alloys have been considered. The present work emphasizes on the preparation of ceramic particulate reinforced aluminium metal matrix composite via spray deposition technique. The

reinforcement chosen for the study is zircon sand, a mineral found in Kerala, Tamilnadu. The prepared composite is further characterized by XRD, optical microscopy, scanning electron microscopy (SEM). For application purposes hardness and wear tests of the synthesized composite was also done.

## CHAPTER-2

### SPRAY FORMING

---

Spray forming, also known as spray casting, spray deposition and in-situ compaction, is a method of casting near net shape metal components with homogeneous microstructures via the deposition of semi-solid sprayed droplets onto a shaped substrate. In spray forming an alloy is melted, normally in an induction furnace, then the molten metal is slowly poured through a conical tundish into a small-bore ceramic nozzle. The molten metal exits the furnace as a thin free-falling stream and is broken up into droplets by an annular array of gas jets, and these droplets then proceed downwards, accelerated by the gas jets to impact onto a substrate [5]. The process is arranged such that the droplets strike the substrate whilst in the semi-solid condition, this provides sufficient liquid fraction to 'stick' the solid fraction together. Deposition continues, gradually building up a spray formed billet of metal on the substrate.

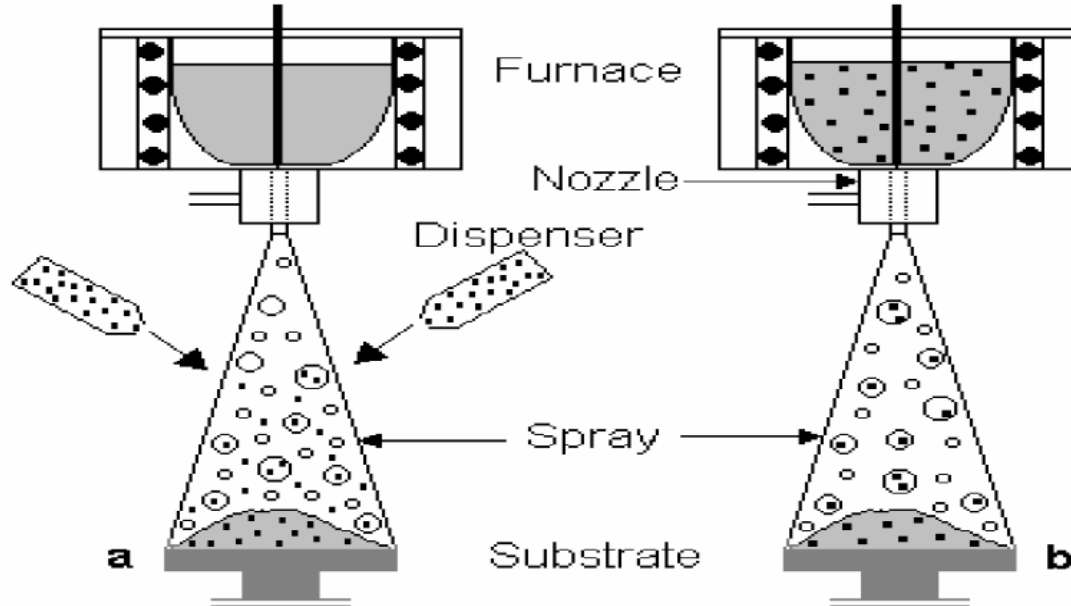


**Fig. 2.1:** Mode of addition of particles (a) through dispenser, (b) premixing in the crucible [3].

Large performs can be produced in a variety of geometries including billets, tubes and strips. The mode of adding particulates are shown in Fig. 2.1. In spray casting a stream of molten metal is

atomized by an inert gas, to form a spray of fine liquid droplets. The atomizing gas removes heat from the droplets and accelerates them towards a moving substrate where they coalesce to form a fully dense deposit. Depending on the motion of the substrate a near net shaped metal component can be fabricated directly from the melt in a single operation. The resulting microstructure is similar to that obtained via rapid solidification or powder metallurgy processing, with fine grain sizes and greatly reduced levels of segregation. Spray forming has found applications in specialist industries such as: stainless steel cladding of incinerator tubes; Ni superalloy discs and rings for aero-engine applications; Al/Ti, Al/Nd and Al/Ag sputter targets; Al-Si alloys for cylinder liners; and high speed steel.

Spray casting is an emerging technology for the fabrication of near net shaped metal components. In origin the process is similar to powder metallurgy (P/M) processing in that a metal part is built up by the consolidation of small droplets or particulates. However, spray casting improves on P/M processing by eliminating a large number of the processing steps required to manufacture a single component. In spray casting a near net shape can be cast directly from the melt in a single operation. The resulting part exhibits a rapidly solidified microstructure with very refined grain sizes and greatly reduced levels of segregation. The ability of the process to eliminate harmful segregation effects makes it a very attractive alternative processing route for those difficult to work alloy systems which cannot be fabricated in the as-cast condition high speed steels [6].

The gas atomized spray forming (GASF) process typically has a molten alloy flow rate of 1–20 kg/min, although twin atomizer systems can achieve metal flow rates of up to 80 kg/min. Special steel billets of 1 tonne or more have been produced by spray forming on a commercial basis, together with Ni superalloy ring blanks of up to 500 kg and Al alloy extrusion billets of up to 400 kg.

## **2.1 History of spray casting**

The process, also known as spray deposition or spray forming, was first developed by Professor A.R.E. Singer and his colleagues at the University of Swansea, Wales in the late 60's and early 70's. The process was later further developed and commercialized by graduate students from Swansea who set up Osprey Metals Ltd. and named the technology "the Osprey process. In the late 70's Sandvic Steel of Sweden realized the potential for making stainless steel tubes by spray

casting and acquired Osprey Metals Ltd. Sandvic are currently building the first full scale plant for commercial operation. Since then the technology has been utilized throughout Europe and Japan, mostly by aluminium companies interested in fabricating metal matrix composites by spray casting. Mannesmann Demag of West Germany have an agreement with Osprey Metals to build and install spray casting equipment around the world. In more recent years U.S. metal manufacturers have been investigating the process.

Professor Nick Grant at M.I.T. has developed a similar spray deposition process known as Liquid Dynamic Compaction (LDC). The main difference between the LDC process and the Osprey process is that an ultrasonic atomizer is used instead of a gas atomizer. Drexel became the first university to investigate the Osprey process, obtaining a small pilot plant unit in 1985. Since then Drexel has conducted a fundamental study of the Osprey process sponsored by ONR (Office of Naval Research) and investigated strip casting of plain carbon steel via spray deposition sponsored by NSF (National Science Foundation) [6].

## **2.2 Atomization**

There are many different techniques for atomization of molten metals, many of which are derived from the powder metallurgy industry. These are:

- (a) Centrifugal atomization
- (b) Gas atomization

### **2.2.1 Centrifugal atomization**

Centrifugal atomization involves pouring molten metal at relatively low flow rates (0.1-2kg/min) onto a spinning plate, dish or disc as shown in Fig. 2.2. The rotation speed of plate is sufficient to create high centrifugal forces at the periphery and overcome surface tension and viscous forces so the melt is fragmented into droplets. Droplet diameters produced by centrifugal atomization are dependent primarily on the rotation speed, (up to 20,000rpm) and are typically in the range 20 – 1000  $\mu\text{m}$  with cooling rates of the order  $10^4 \text{ K s}^{-1}$  . Centrifugal atomization is generally conducted under an inert atmosphere of Ar or  $\text{N}_2$  to prevent oxidation of the fine droplets or can be operated under vacuum [5].

The gas assisted spray forming processes are the most well developed, attracting world-wide interest for the processing of Al, Ni and Fe based alloys. The process is economically

constrained by the post-spray processing problems due to gas entrapment and thermal induced porosity in the product.

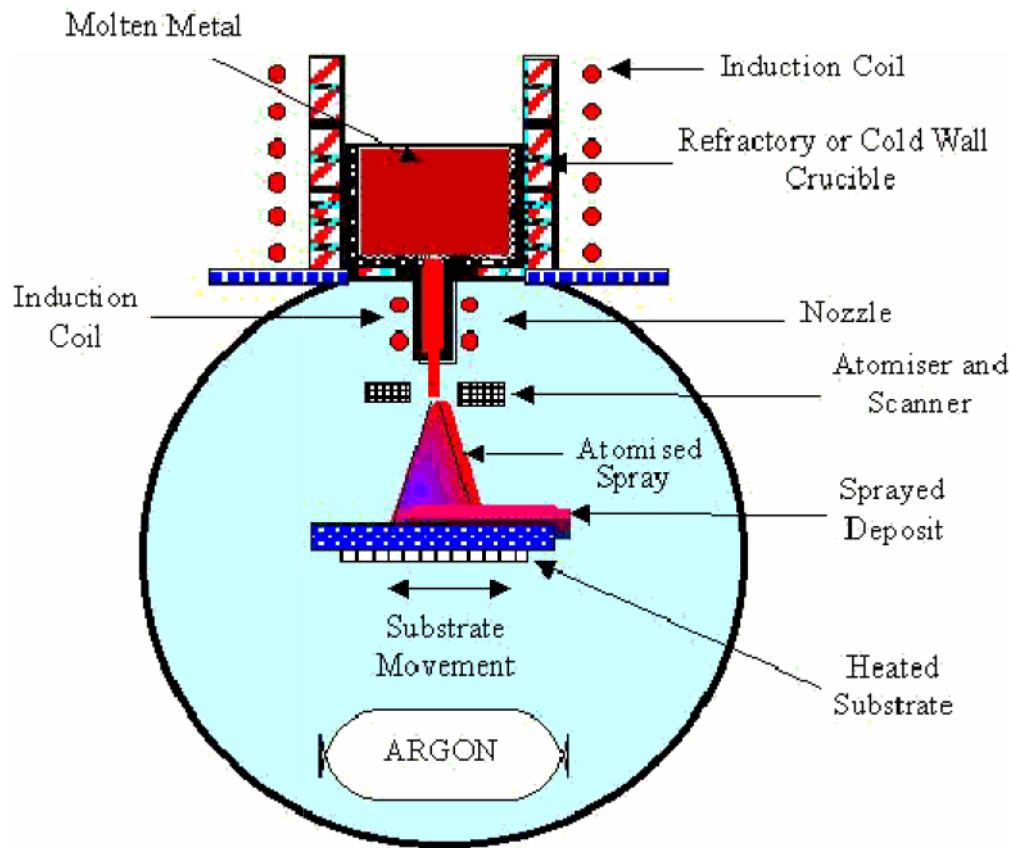


**Fig. 2.2:** Systematic representation of centrifugal atomization [5].

In centrifugal spray deposition (CSD) atomization is achieved by the interaction of a fine stream of liquid metal with the surface of a rapidly rotating disc. The centrifugal forces associated with disc rotation act to disperse the liquid into a fine spray of droplets which are directed on to the internal surface of a ring shaped collector which is reciprocated in the path of the spray. Careful control of the liquid metal flow rate to the cup, the speed of cup rotation and the mode and rate of substrate motion allows the production of ring shaped preforms with complex internal and external shape. Since gas is not instrumental to the process the system can be operated under vacuum with inherent cost and metallurgical benefits. The centrifugal atomization and deposition equipment currently being used and have the ability to produce ring shaped preform with external diameters ranging up to approximately 1.10m and axial height varies up to 0.20m.

### 2.2.2 Gas atomization

In gas atomization, the kinetic energy of an impinging high velocity gas jet disintegrates the continuous metal flow into droplets.

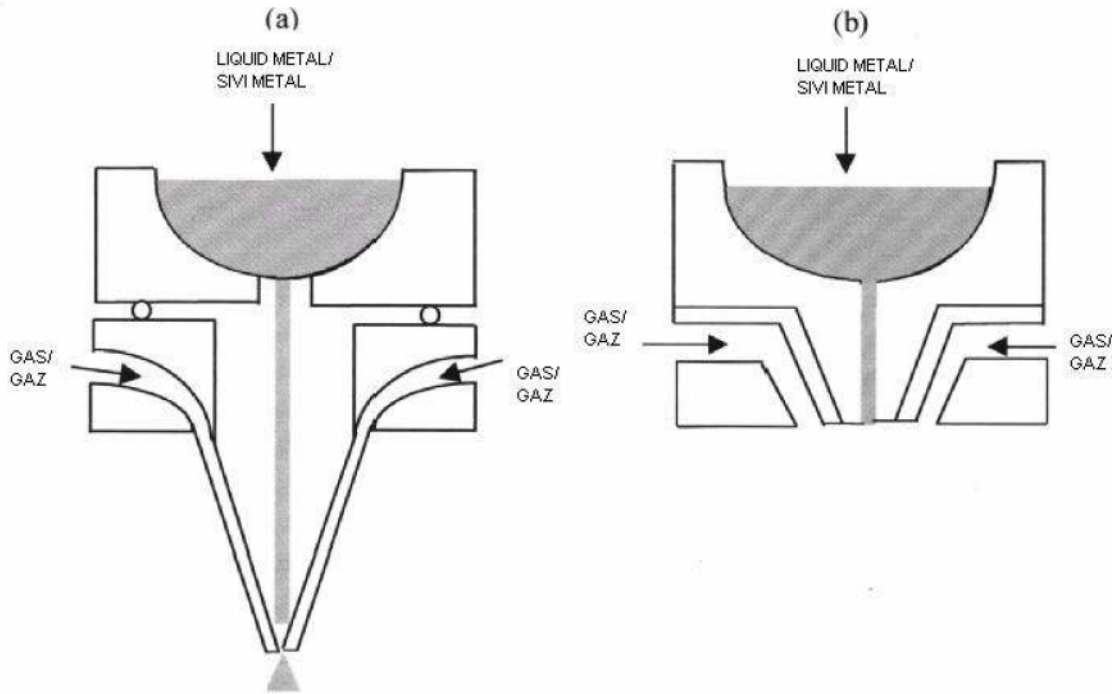


**Fig. 2.3:** Schematic of (a) free fall or open atomizer, and (b) a closed coupled or closed atomizer [7].

There are essentially two kind of gas atomizer, as shown schematically in Fig. 2.3(a) and Fig. 2.3(b). In free fall or open atomizers in Fig. 2.3(a), the melt falls unconstrained into a region where atomization occurs. In close coupled or closed atomizers in Fig. 2.3(b), the gas atomizes the metal directly on exit from the melt delivery nozzle. The gas kinetic energy is consequently higher in comparison with open atomizers and gives powders of smaller median diameters. However, because the tip of the melt delivery nozzle is chilled by the flow of the cool atomizing gas in closed atomizers, freezing of the metal may occur before atomization (freeze off) and closed designs are generally only used in conjunction with low melting point materials where the temperature difference between melt and gas is relatively small.

Open and closed atomizers as shown in Fig. 2.3(a) and Fig. 2.3(b) may be further subdivided into annular types, in which the gas exit is a continuous circular slit as shown in Fig. 2.4(a), and those using a ring of circular gas exits, as shown in Fig. 2.4(b). In linear atomizers, a series of circular gas exits that are arranged either side of a melt delivery slit, as shown in Fig. 2.4(c). Several linear atomizers can be used to atomize a sheet of droplets for the production of wide strip.

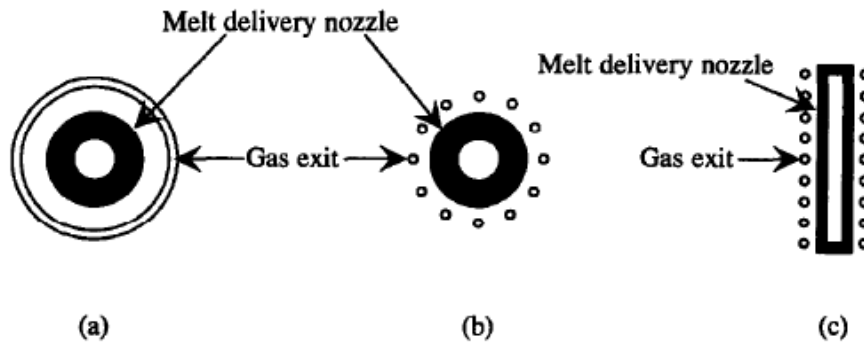


**Fig. 2.4:** Schematic of (a) an annular atomizer, (b) a multi jet atomizer and (c) a linear atomizer [4].

Secondary gas jets may be used either to shroud the molten metal stream prior to atomization or to restrict spray divergence of the droplet spray after atomization. Droplet spray scanning is used to average spatial variations in spray density and droplet size over the preform surface and allow large diameter preforms (up to 350 mm) to be manufactured. Scanning is achieved either by an alternating gas flow from opposing jets (Fig. 2.5(a)) or by mechanical oscillations of the atomizer (Fig. 2.5(b)).

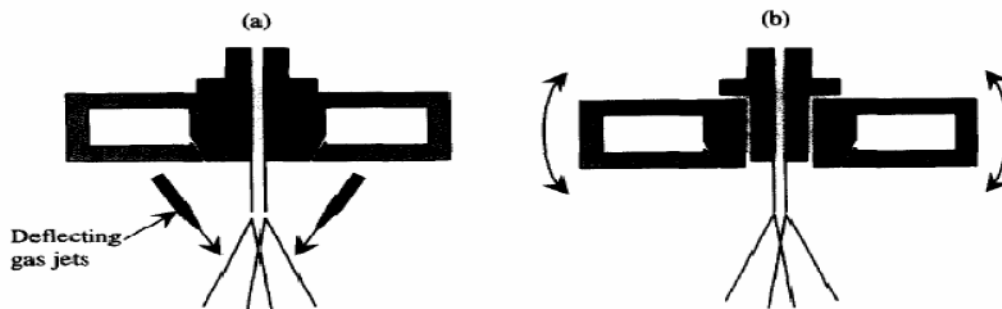


**Fig. 2.5:** Schematic of (a) pneumatic and (b) mechanical scanning atomizer arrangement [4].

Spray deflections of 5-10° at frequencies of up to 25 Hz are achievable. For larger preform diameters up to 450 mm where the required spray scan angle and corresponding changes in preform/atomizer separation become too large, twin or multi-atomizers simultaneously spraying onto a single preform have been suggested.

Twin atomizer systems also offer the benefits of increased production rates, improved gas consumption and increased yield, as shown in Table 2 for high speed steels.

**Table 2** A comparison of single and twin atomizers for spray deposition of high speed steel billets [4].

Material Properties	Single atomizer	Twin atomizer
Billet diameter (mm)	150	Up to 450
Metal flow rate (kg/min)	24	30
Gas consumption (m <sup>3</sup> /kg)	1	0.75
Deposition yield (%)	61	80
Depth of surface porosity (mm)	8	< 2

The melt stream exits the melt delivery nozzle into the spray chamber. The melt stream is protected from being destabilized by the turbulent gas environment in the spray chamber by primary gas jets operating at intermediate inert gas pressure of 2 to 4 bar, the resulting gas flow is parallel to the melt stream to stabilize the melt stream. The secondary atomizer uses high velocity (250 to 350 ms<sup>-1</sup>), high-pressure (6 to 10 bar) gas jets to impinge on the melt stream to achieve atomization. The atomizer jets are usually arranged as an annulus or as discrete jets positioned symmetrically about the melt delivery nozzle, or less commonly, arranged as a linear nozzle for the production of strip products. Typical droplet diameters follow a log-normal distribution with powder diameters up to ~600 μm with a mass median diameter of ~150 μm.

The atomizing gas mass flow rate to molten metal mass flow rate ratio is a key parameter in controlling the droplet diameter and hence the cooling rate, billet temperature and resulting solid particle nucleant density. The gas - metal ratio (GMR) is typically in the range 1.5 to 5.5, with yield decreasing and cooling rates in the spray increasing with increasing GMR. Typically at low

(1.5) GMR, yield is 75%, if the GMR is increased to 5.0 with all other parameters remaining constant, the process yield is reduced to 60%.

Scanning atomizers have been developed which allow the production of billets of up to 600 mm diameter, approximately twice the diameter possible with a static atomizer. The atomizer head is oscillated mechanically through 5 to 10° at a typical frequency of 25 Hz, to deflect the melt stream creating a spray path that is synchronized with the rotation speed of the collector plate in order to deposit a parallel-sided billet. By using programmable oscillating atomizer drives it was possible to improve the shape and shape reproducibility of spray formed deposits. It has been demonstrated that parallel sided, flat topped billets could be sprayed in a reproducible manner if the substrate rotation and atomizer oscillation frequency were synchronized and optimized for specific alloys and melt flow rates. Twin atomizer systems combine a static and scanning atomizer, making it possible to spray billets of up to 450 mm diameter with economic benefits.

Atomizing gas used in spray forming is generally either N<sub>2</sub> and can be either protective or reactive depending on the alloy system, or Ar which is generally entirely inert but more expensive than N<sub>2</sub>. Reactive gasses can be introduced in small quantities to the atomizing gas to create dispersion strengthened alloys e.g. 0.5 – 10 % O<sub>2</sub> in N<sub>2</sub> used to generate oxide dispersion strengthened (ODS) Al alloys. Comparisons of N<sub>2</sub> and Ar based spray forming showed that with all other factors remaining constant, the billet top temperature was lower with N<sub>2</sub> than with Ar, because of the differences in thermal diffusivity of the two atomizing gases: Ar has a thermal conductivity of 0.0179 W/mK which is approximately a third less than N<sub>2</sub> with a thermal conductivity of 0.026 W/mK.

### **2.3 Mechanisms of atomization**

The mechanisms of melt break up and atomization has been extensively researched showing that three important stages are responsible for the disintegration of a liquid sheet in to droplets. These stages are:

- (1) Formation and growth of disturbance waves in the liquid,
- (2) Disruption of liquid sheet in to fragments, and
- (3) Formation of droplets by the further breakup of fragments.

First, waves initiate on the liquid sheet as a result of the disturbances that are imposed by the ambient atmosphere or the atomization media. The variation of air pressure and the shear force

generated by the relative velocity at the gas-liquid interface cause some of these waves to grow in amplitude as a function of time and the distance from the nozzle exit. Second, when the most rapidly growing waves reach some critical amplitude the sheet of liquid with ripples and protuberances becomes unstable. At this point, fragments are torn off from the liquid sheet at the crests and troughs. Third, liquid fragments become unstable under the aerodynamic and surface tension forces and further break down into ligaments. Finally, droplets are formed by the spheroidization of ligaments under the action of surface tension forces.

The twin fluid atomization of liquids may be more complex, for this the conventional atomization of a molten metal may consist of five distinct stages. These stages are

- (1) Formation of waves from initial disturbances,
- (2) Formation of fragments from the liquid,
- (3) Formation of droplets by the disintegration of fragments,
- (4) Breakup of large droplets, and
- (5) Coalescence of droplets during collision.

In stage 1, waves form in the liquid as a result of the initial disturbances that are present on the surface of the liquid. There are several proposed origins of the initial disturbances. For example, it has been suggested that the most important disturbances are generated inside of the delivery tube. Turbulence can be generated inside a delivery tube by flow separation at sharp corners, wall roughness, boundary layers and shear flow. In stage 2, the amplitude of the growing waves reaches a critical value. In this stage fragments with relatively large aspect ratios are torn off from the disturbed liquid. In stage 3, the fragments that were torn off from the liquid during stage 2 become unstable and droplets are formed by the subsequent breakup and spheroidization of liquid fragments. The droplets formed during stage 3 may be subjected to further breakup when their size is greater than a certain critical value. Accordingly, for droplets that are large than the critical size (critical droplet size may be defined as the smallest size of droplets which is unstable under the pressure and shear forces that are imposed by the atomization environment.), the aerodynamic forces that are generated due to relative velocity between gas and droplets may exceed the restoring force arising from surface tension. In stage 4, the droplets that are greater than a critical size experience further deformation, becoming first flat and then bowl shaped. The resultant liquid with a bowl-like geometry eventually bursts into droplets of smaller sizes. Since in this stage, new droplets are formed by the breakup of coarse droplets that were formed earlier,

this particular stage is also referred to as secondary atomization. In stage 5, collisions occur between droplets which formed during the early stages, leading under certain conditions, to droplet coalescence [8].

## 2.4 Deposition and preform solidification

Models and experimental measurements show that small droplets (<50 μm) very rapidly become fully solid prior to deposition, 50-200 μm droplets will be typically semi-solid and droplets of diameters >200 μm will be liquid at deposition. The range of droplet dynamic and thermal histories results in a billet top surface of 0.3 to 0.6 solid fractions. Some solid droplets will bounce or splash-off the billet top surface or be directed out of the deposition region by turbulent gas movement in the chamber. The proportion of droplets that impact the surface compared to the proportion that are incorporated into the billet has been termed the ‘sticking efficiency’.

Droplets which impinge on the preform surface may be either fully liquid, mushy or fully solid, and the substrate surface itself may also be fully liquid, mushy or solid. The combination of droplet and preform solid fractions determines the way in which droplets either bounce off the preform or are incorporated. The overall top surface solid fraction is determined by the relative rates of heat input into and output from the preform top surface. The heat input rate is determined by the average enthalpy of the droplet spray and its mass arrival rate on the preform top surface. The heat output rate is determined by convective cooling conditions, preform thermal conductivity and thermal gradients [4]. The balance between heat input and output rates and the subsequent macroscopic preform heat flow control the evolution of the spray formed microstructure.

**Table 3** Relationship between spray conditions, preform condition and deposition behavior during spray forming [2].

		Spray Condition		
		Solid	Mushy	Liquid
Preform Condition	Solid	bounce off	partial sticking	good sticking
	Mushy	partial sticking	good sticking	good sticking
	Liquid	Surface ejected and whipped up	Surface ejected and whipped up	Surface ejected and whipped up

## 2.5 Metallurgical characteristics of spray formed alloys

Although the solidification rates in spray casting are high, equal to  $10^3$ - $10^4$  K s<sup>-1</sup>, it should be noted that solid state quenching is relatively slower than in the powder metallurgy process. It is possible to achieve a fine and homogeneous microstructure, increased solid solubility of alloying elements and decreased segregation with rapid solidification. During spray casting, the characteristics of the rapid solidification process are observed, but to a lesser degree. For example, although fine precipitates are produced when spray forming, they are coarser than those produced in powder metallurgy. Generally, spray formed alloys show the following characteristics:

- High-density preforms, typically 96-99% of theoretical, are produced.
- Oxygen content is decreased, compared to P/M products, and degassing operations are not needed.
- Rapid solidification results in a fine, uniform grain size, typically in the range 20-50  $\mu\text{m}$ .
- As a result of rapid solidification, macrosegregation is sharply decreased.
- Fine precipitates are produced and uniformly distributed in the microstructure. Although precipitation in the liquidus/solidus region occurs very rapidly, any solid-state transformations are relatively slow.
- Superior fracture properties are obtained in comparison to P/M and I/M products. There are two reasons for this:

- i) Decreased oxidation compared to P/M;
- ii) Absence of coarse precipitates compared to I/M [7].

## 2.6 Spray formed microstructure

During spraying it is essential to maintain a constant top surface temperature and hence maintain steady-state conditions if a billet with consistent microstructure is to be produced. At the billet surface, during spraying an enthalpy balance must be maintained. The rate of enthalpy lost  $H_{\text{out}}$  from the billet by conduction to the atomizing gas and through the substrate; convection and radiation must be balanced with the rate of enthalpy input  $H_{\text{in}}$  from the droplets in the spray. There are a variety of factors that can be adjusted in order to maintain these conditions: spray height, atomizer gas pressure, melt flow rate, melt superheat and atomizer configuration, being those parameters most readily adjusted. Typically equipment such as closed circuit cameras and

optical pyrometry can be used to monitor billet size / position and top surface temperature. If  $H_{out} \gg H_{in}$  then a steady temperature is maintained at the billet top surface. The top surface should be in a mushy condition in order to promote sticking of incoming droplets and partial re-melting of solid particles. The necessary partial re-melting of solid droplets explains the absence of dendritic remnants from pre-solidified droplets in the final microstructure.

The final phase of solidification occurs once droplets have impacted the mushy billet surface and thermal equilibration has taken place between the droplets and the billet. At this stage residual liquid is present as continuous network delineating polygonal grain boundaries, with a typical liquid fraction of 0.3 – 0.5 [5]. Fig. 2.6 shows a typical polygonal of spray formed Ni superalloy billet.

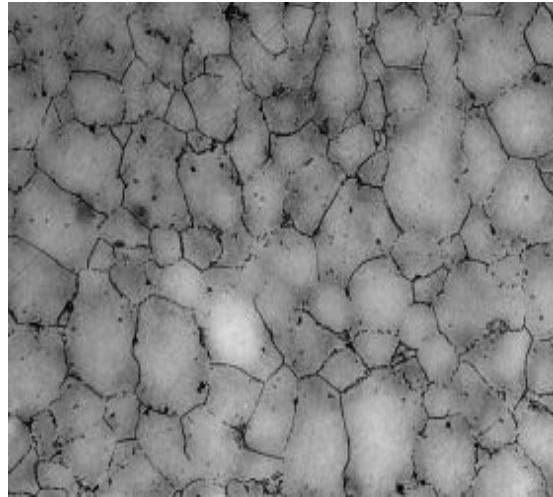


**Fig. 2.6:** Typical polygonal as spray formed Ni superalloy billets [9].

Although one of the benefits of spray forming is purportedly the ability to produce bulk material with fine scale micro segregation and little or no macro segregation work on Al-Mg-Li-Cu alloys showed that as a consequence of the interconnected liquid in the billet there was significant macro segregation in large spray formed wrought Al billets. The distribution of Cu, Mg and Li in, for example, Al alloy 8091 showed surprisingly pronounced macro segregation with the variation of Cu (wt%) in a spray formed 8091 billet, ranging from ~1.4 at the billet centre to 1.92 at the billet periphery. These macro segregation patterns were explained in terms of inverse segregation in which solute rich liquid from the billet centre is sucked back through the primary Al-rich network to feed solidification shrinkage at the billet periphery. This effect was suggested to be exacerbated by centrifugal effects from the billet rotation.

As sprayed the billet porosity is typically 1-2% with a region of higher porosity in the splat-quenched region adjacent to the substrate. The very top of the billet often shows increased porosity because the top is rapidly chilled by the atomizing gas which continues to chill the billet for 10-60 s after spraying. There has also been little progress in understanding and quantifying the underlying physics that controls as-sprayed porosity. In most cases, the higher porosity at the billet base and top are scalped and recycled. Ultrasonic inspection is sometimes used to determine the depth of the chill zone regions to prevent unnecessary wastage. Depending on the alloy system and the final application, the remaining bulk material is usually processed to close porosity and subjected to a range of thermo-mechanical treatments. Spray formed materials are rarely used in the as-sprayed condition and are often treated by hot isostatic pressing (HIPing) to remove porosity. In some cases, the residual atomizing gas in pores may react with alloying elements to form allegedly beneficial phases e.g. N<sub>2</sub> reacting with Ti in Ni superalloy Rene 80 to form a dispersion of TiN.

## 2.7 Application

The range of products currently being manufactured covers a broad spectrum of shapes, alloys, and markets, including round billets, tubes, rings, and clad products; Al, Cu, Ni, Fe, and Si-based alloys; and automotive, electronics, aerospace, and general engineering components. Currently, the main applications for spray forming are:

- (1) *Aluminium-alloy billets*: Installed manufacturing capacity is 3,500 t/y at Peak (Germany), 1,000 t/y at Sumitomo Light Metals (Japan), and 400 t/y at Osprey Metals (United Kingdom). Peak is manufacturing Al/Si alloy billets for subsequent conversion into cylinder liners for use in automotive engines. More specialist, high-strength (Al/Zn), high-temperature (Al/Cu), and light-weight alloys (Al/Li) and metal-matrix composites (MMCs) are produced at Osprey Metals, mainly in conjunction with Peak. Kobelco has also recently announced the commercialization of special aluminium alloys for use as sputter target materials.
- (2) *Copper-alloy billets*: The combined manufacturing capacity at Swissmetall Boillat (Switzerland) and Wieland (Germany) is in excess of 2,000 t/y, but presently only part of this capacity is being utilized. One of the main products for which there is

considerable growth potential is electronic connectors, particularly for use in "high-tech" telecommunication applications.

- (3) *Spray-formed connectors*: produced by Swissmetall are already starting to replace wrought Cu-Be alloys and P/M Cu-Ni-Sn alloys.
- (4) *Special steel and superalloy billets*: A new plant recently installed at Danspray (a subsidiary of Danish Steel, Denmark) for high-alloy steels has a single-shift capacity of 2,000 t/y and will be used for producing both ingot-metallurgy alloys, such as D<sub>2</sub> tool steel, and P/M-type alloys, such as T<sub>15</sub> high-speed steel. Superalloy billets are presently manufactured in a pilot plant at Osprey Metals for evaluation by Allvac SMP (United Kingdom). A pilot facility for producing billets from a refractory-free melt source is under development at General Electric (United States) in conjunction with Allvac (United States) for turbine discs applications.
- (5) *Superalloy rings*: Rings, seals, and cases for use predominantly in aircraft gas-turbine engines are being manufactured by Sprayform Technologies International (a Howmet/Pratt and Whitney joint venture company). A new plant recently installed at Sprayform Technologies (United States) has a manufacturing capacity of 500t/y (single shift) using a three-tonne vacuum-induction melting (VIM) furnace. Stainless steel and nickel-alloy tubes and composite tubes. Sandvik Steel (Sweden) operates a plant with a capacity of approximately 750 t/y (two shifts), where one of the main products is composite tubing for use in municipal waste incinerator plants
- (6) *Rolls and clad rolls*: Small-section mill rolls continue to be spray formed by Sumitomo Heavy Industries Foundry and Forgings (Japan). Clad rolls, which are produced on a development basis only at Osprey Metals, are being evaluated at Sheffield Forgemaster Rolls (United Kingdom).
- (7) *Silicon-aluminium alloys*: A unique series of alloys are being produced by Osprey Metals for use in electronic packages, heat sinks, and other applications where lightweight materials with a low coefficient of expansion are a requirement [9].

## 2.8 Advantages

1. Spray forming offers certain advantages over both conventional ingot metallurgy and more specialist techniques such as powder metallurgy.

2. It is a flexible process and can be used to manufacture a wide range of materials, some of which are difficult to produce by other methods, e.g. Al-5wt%Li alloys or Al-SiC, Al-Al<sub>2</sub>O<sub>3</sub> metal matrix composites (MMCs).
3. The atomization of the melt stream into droplets of 10-500µm diameter, some of which, depending on diameter, cool quickly to the solid and semi-solid state provide a large number of nucleants for the residual liquid fraction of the spray formed material on the billet top surface.
4. The combination of rapid cooling in the spray and the generation of a large population of solid nucleants in the impacting spray leads to a fine equiaxed microstructure, typically in the range 10-100µm, with low levels and short length scales of internal solute partitioning.
5. These micro structural aspects offer advantages in material strength because of fine grain size, refined distribution of dispersed and / or secondary precipitate phases, as well as tolerance to impurity 'tramp' elements.
6. One of the major attractions of spray forming is the potential economic benefit to be gained from reducing the number of process steps between melt and finished product.
7. Spray forming can be used to produce strip, tube, ring, clad bar / roll and cylindrical extrusion feed stock products, in each case with a relatively fine-scale microstructure even in large cross-section [5].

## **2.9 Disadvantages**

There are two major disadvantages to the gas atomization spray forming process.

1. The major disadvantage is one of process control. As it is essentially a free-forming process with many interdependent variables, it has proved difficult to predict the shape, porosity or deposition rate for a given alloy.
2. Porosity resulting from gas entrapment and solidification shrinkage is a significant problem in spray formed materials. A typical spray formed billet will contain 1-2% porosity with a pore size dependent on alloy freezing range and various process parameters. Hot isostatic pressing (HIPing) or thermo-mechanical processing can heal these pores if they are small (<30µm) [5].

## 2.10 Commercialization

In spite of the problems associated with the spray forming process there has been sustained industrial interest in spray forming over the last ~35 years. Sandvik-Osprey (former Osprey Metals Ltd) of Neath, South Wales holds the patents on the process and have licensed the technology to a range of industries. There are currently ~25 licensees operating around the world, ranging from small research and development plants to full-scale commercial operations. These include successful commercial ventures such as PEAK (Germany) who currently spray form Al-Si cylinder liners for Mercedes Benz; Danspray (Denmark) producing specialist tool steels; and Sandvik Steel producing stainless steel clad tubes for incinerator applications. Wieland-Werke AG (Germany) spray form copper alloys which are difficult to cast and tend to strong segregation. Main applications are prematerial for low temperature Nb<sub>3</sub>Sn superconductors (CuSn), oil drilling equipment (high strength material CuMnNi) and for forming tools (CuAlFe with high Al-content). Research and development activities include: Pennsylvania State University (USA), investigating high strength Al alloys for defence applications and Oxford University investigating Ni superalloys, Al-Si and Al-Li alloys, and others. In all of these applications, research concerns the reconciliation of the cost disadvantages and complexity of spray forming with demand for high performance alloys in niche applications [5].

## **CHAPTER-3**

### **LITERATURE REVIEW**

---

Kimirami et al. [10] have studied the formation of novel microstructure by spray deposition process. Due to relatively high cooling rate, the characteristic microstructure of as-spray deposits typically consist of a fine scale microstructure and also exhibit some extended solid solubility and metastable phases. They have studied alloys of several different systems with the aim of investigating the potential of achieving the formation of novel microstructures by the high cooling rate involved in the near-net-shape process and found that the spray deposition is a very interesting near-net-shape process for achieving novel microstructures in a variety of alloy systems.

K. Raju et al. [11] have summarized the work carried out in the area of spray forming of aluminium alloys and its composites. In this article, main emphasis was given to the microstructures, wear characteristics, and mechanical properties of as-cast and as-sprayed aluminium alloys. Also, this article is designed to provide the microstructures of as-cast and as-sprayed Al-15%Si alloy. The microstructure of as-sprayed alloy has invariably indicated equiaxed grains throughout the deposit and has been observed that the Si particles are uniformly distributed in the Al matrix. Spray forming offers a combination of low cost manufacturing with enhanced properties and performance. As such it has emerged as a key competitor for existing technologies such as conventional casting, ingot metallurgy, and powder metallurgy.

Srivastava et al. [12] investigate the microstructural characteristics and mechanical properties of Al-6.5Si and Al-18Si alloys. The microstructure of the spray deposit of Al-6.5Si alloy showed spherical morphology of the primary  $\alpha$ -phase with a globular shape of the eutectic Si phase in the inter-particle boundaries. On the other hand a fine particulate morphology of primary Si phase uniformly dispersed in the matrix of the  $\alpha$ -phase was observed in spray-deposit of Al-18Si alloy. Microstructural refinement was further increased in the hot extruded alloys. The room temperature tensile tests of spray formed and extruded alloys showed considerable increase in their strength and ductility over that of the as cast alloys.

Satyanarayana et al. [13] have studied on spray casting of Al-alloys and their composites. A spray nozzle of convergent–divergent configuration was used for spray castings (SC) of A16061/LM25 alloys and their composites. Both monolithic alloys and composites showed equiaxed fine grained microstructure with a variation in grain size from 20 to 30  $\mu\text{m}$ . Some of the regions of the preform also showed cellular solidification structure with globularization of most of the eutectic Si suggesting the effect of rapid solidification observed with bulk samples showing uniformly distributed porosity. TEM studies showed decoration of grain boundaries/presolidified droplets by some precipitates and also vacancy loops. Their aging characteristics indicated lowering of solutionising temperature and aging time to get the same peak hardness as obtained in the alloy produced by ingot metallurgy methods. An ordered phase with unit cell four times larger than Al seems to form during the in situ heating of LM25–SiC samples while dislocations seem to emerge from the interface between the particle and the matrix.

Lavervia [14] has studied the synthesis of discontinuously reinforced Metal-matrix composites using spray atomization and co-injection. A variety of processing techniques have evolved over the last two decades to optimize the structure and properties of particulate reinforced metal-matrix composites (MMCs). Among these, spray processes offer a unique opportunity to combine the benefit associated with fine particulate technology with in situ processing, and in some cases, near-net shape manufacturing. Spray processing generally involves mixing reinforcements and matrix under highly non-equilibrium conditions, and as a result, these processes offer the opportunity to modify the properties of existing alloy systems, and develop novel alloy compositions. In principle, such an approach will inherently avoid the extreme thermal excursions, with concomitant macrosegregation, normally associated with casting processes. Furthermore, this approach also eliminates the need to handle fine reactive particulates, normally associated with powder metallurgical processes.

Yan et al. [15] have studied an aluminium alloy metal matrix discontinuously reinforced with silicon carbide particulates which was synthesized using the spray atomization and co-deposition technique. Microstructural characterization studies were performed to provide an understanding of the intrinsic effects of carbide particulate co-injection in to the aluminium alloy metal matrix. The results reveal the ageing kinetics to be altered by the reinforcing ceramic particulates.

Ambient temperature tensile tests revealed that the presence of particulate reinforcement in the aluminium alloy metal matrix degrades both strength and ductility.

Pandey et al. [16] have employed the gas atomization technique to produce Al-Si powders. The 45 micron size spherical shape particles are obtained in contrast to oblong shape coarse particles. The microstructural examination of powders invariably revealed microcellular, cellular and dendritic morphologies of the primary phase. Depending on the size of the particles; considerable supersaturation of silicon in the aluminium matrix was observed particularly in fine powders. The cooling rate of particles estimated from dendrite arm spacing and a heat transfer model was observed to vary in the order of  $10^3$ - $10^5$ k/s.

Chaudhury et al. [17] have synthesized aluminium based metal composites by a new spray forming technique. In their investigation, Al-2Mg-7TiO<sub>2</sub> composite was successfully spray atomized and co-deposited on a rotating substrate. The authors describe the processing methodology for the fabrication of Al-TiO<sub>2</sub> composites, which involves simultaneous introduction of aluminium melt and rutile particles through concentric tubes followed by inert gas atomization and deposition on a rotating copper substrate placed vertically below the atomiser at some predetermined height. Mechanical and physical properties of as-cast and composite materials are discussed. For comparison, Al-2Mg-5TiO<sub>2</sub> composite was also prepared by stir cast method and characterized.

Gupta et al. [18] have investigated the microstructure, thermal stability and elevated temperature mechanical behavior of Al-Ti-SiC metal matrix composites processed by spray atomization and co-deposition. The evolution of the microstructure of the spray-deposited material before and after thermal annealing was studied using X-ray diffractometry, TEM, SEM and optical microscopy. The thermal stability of the spray-deposited materials was determined by monitoring the changes in hardness after isochronal thermal anneals at various temperatures. The results of X-ray and microanalysis studies revealed the presence of a supersaturated solid solution. The formation of an extended solid solution was discussed. The results suggest that the as-spray deposited and hot extruded Al-Ti matrix is thermally stable up to a temperature of 400°C. The excess solid solubility of Ti in -Al is maintained up to a temperature of 300°C during the process. The elevated-temperature mechanical properties of the hot extruded spray-deposited materials were studied following a 100-hour exposure at 250°C, 350°C, and 450°C.

The results show that the elevated-temperature yield strength of the spray-deposition and extruded materials compared favorably to those of an equivalent alloy made by powder metallurgical materials, were superior to those of the ingot material but were inferior to those of mechanically alloyed Al-Ti materials.

Santos et al. [19] have studied the corrosion behaviour of a hypereutectic Al-Si alloy obtained by spray forming in acid, neutral and alkaline solutions. Al-Si hypereutectic alloys produced by spray forming represent an important technological development for application in the aeronautical and automotive industries. Due to some special properties these alloys find application as cylinder liners, mainly due to their high strength and wear resistance. Much research has been carried out to evaluate the mechanical properties of these alloys but the literature on their corrosion performance is still very scarce.

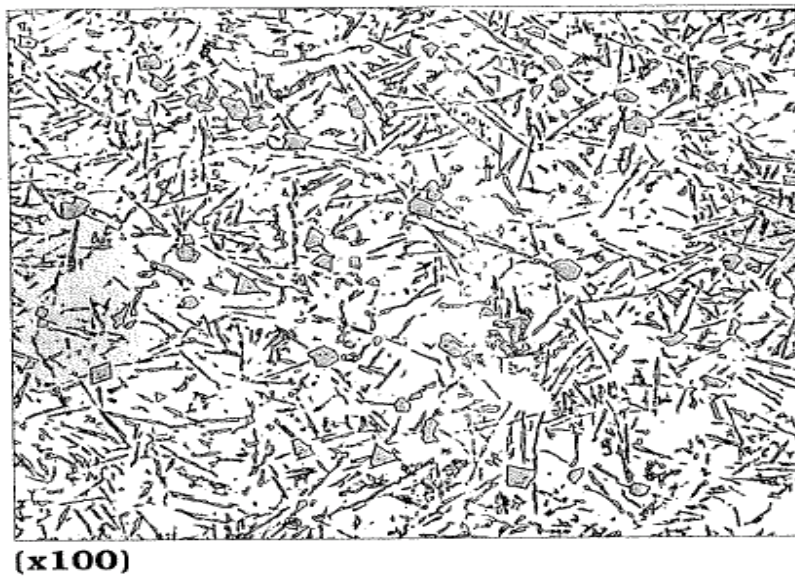


**Fig. 3.1:** Micrograph of Al-Si (hypereutectic alloy)

In this study, the corrosion behaviour of a spray formed Al-Si-Cu hypereutectic alloy was investigated by electrochemical impedance spectroscopy (EIS) in acid (pH 3.3), neutral (pH 7) and alkaline (pH 11) solutions. Intense localized attack occurred in the acid electrolyte and the impedance decreased with time of immersion. In the neutral medium, the alloy was passivated but localized attack also occurred on weak areas of the passive film. In the alkaline medium, precipitation of corrosion products occurred during the first hours of immersion causing the

increase of impedance but thickening of this layer led to cracks growth with time and, consequently, to the exposure of metallic substrate, resulting in the decrease in impedance for longer periods..

Jones [20] has studied the formation of microstructure in rapidly solidified materials and its effect on properties. The capability of rapid solidification to generate refined microstructures containing extended equilibrium and non-equilibrium constituents has been known for decades, but it is only relatively recently that progress has been made in predicting the microstructural outcome of particular sets of rapid solidification conditions. The present contribution reviews the progress made which has involved advances both in theoretical modeling of phase formation and growth kinetics and in the formulation and execution of experimental studies in which the conditions applicable at the solidification front are controlled and known.

Kurz et al. [21] have studied the selection of microstructures in rapid solidified processing. A great variety of microstructures may be observed in an alloy when the solidification conditions and the composition are changed. A criterion for the selection of a given microstructure is presented which is based on comparison of the relevant interface response functions and on the assumption of maximum interface temperature.

Ferrarini et al. [22] have studied the microstructure and mechanical properties of spray deposited hypoeutectic Al-Si alloy. The microstructure and the tensile properties of an Al-8.9 wt.% Si-3.2 wt.% Cu-0.9 wt.% Fe-0.8% Zn alloy processed by spray forming was investigated. The alloy was gas atomized with argon and deposited onto a copper substrate. The microstructure was evaluated by optical microscopy (OM), scanning electron microscopy (SEM) and energy dispersive X-ray spectroscopy (EDS). Small faceted dispersoids observed surrounding equiaxial  $\alpha$ -Al matrix were identified by SEM-EDS as silicon particles. Sand cast samples with the same composition showed a columnar dendritic  $\alpha$ -Al matrix, Al-Si eutectic, polyhedral  $\alpha$ -AlFeSi and needle-like  $\alpha$ -AlFeSi intermetallics. In the spray formed material the formation of the Al-Si eutectic was suppressed, and the formation of the  $\alpha$ -AlFeSi and  $\beta$ -AlFeSi intermetallics was strongly reduced. The fine and homogeneous microstructure showed an aluminium matrix with grain size ranging from 30 to 40  $\mu\text{m}$ , and particle size of the silicon dispersoids having a mean size of 12  $\mu\text{m}$ . Room temperature tensile tests of the spray formed alloy showed relative increasing of strength and elongation when compared with the values

observed for the conventionally cast counterparts. These results can be ascribed to the refined microstructure and the scarce presence of intermetallics of the spray formed material.

Salamci [23] has studied the mechanical properties of spray deposited and extruded 7XXX series aluminium alloys. Mechanical properties of spray deposited and extruded 7XXX series aluminium alloys were investigated in peak aged condition. To study the influence of Zn additions on the mechanical behaviour of spray deposited materials, three alloy compositions were selected namely: SS70 (11.5% Zn), N707 (10.9% Zn) and 7075 (5.6% Zn). After ageing treatment, notched and unnotched specimens of spray deposited alloys were subjected to tensile tests at room temperature. Experimental results showed that the SS70 alloy exhibited the highest strength. Spray deposited Al alloys showed a very high strength as compared to conventionally processed 7XXX series Al alloys. Also spray formed 7XXX series Al alloys give higher fraction toughness as compared to PM processed alloys.

Wang et al. [24] have studied the effect of Si content on the dry sliding wear properties of spray deposited Al-Si alloy. In this investigation, Al-12Si, Al-20Si and Al-25Si (wt.%) alloys were synthesized by spray atomization and deposition technique. The wear resistance of the alloys was studied using a pin-on-disc machine under four loads, namely 8.9, 17.8, 26.7 and 35.6 N. The microstructures, worn surfaces and the debris were analyzed in a scanning electron microscope. It has been found that the effect of Si content on dry sliding wear of spray-deposited Al-Si alloy was associated with applied loads. At lower load (8.9 N), with increasing Si content, the wear rate of the alloy was decreased. At higher load (35.6 N), spray-deposited Al-20Si alloy exhibited superior wear resistance to the Al-12Si and Al-25Si alloys.

Gupta et al. [25] have studied the sliding wear resistance of Al-alloy particulate composites. Two alloy systems were used, One a conventional wear resistant alloy (2014) and the other a non-conventional alloy (7075). It was seen that the 7075 series exhibit higher improvement in wear resistance over the base alloy as compared to the 2014 series. Also in the 2014 alloy system the composites deteriorate faster than the alloy.

Suersha et al. [26] have studied the effect of addition of graphite particulates on the wear behavior in aluminium-silicon carbide-graphite composites. They conclude that increase of speed

reduces wear by supporting mechanically mixed tribo layer and increase of load increases wear by reducing the role of tribo layer.

Wang et al. [27] have compared the sliding wear behavior of a hypereutectic Al-Si alloy prepared by spray-deposition and conventional casting methods and it has been found that the spray-deposition technique produces a finer matrix structure. The spray-deposited alloy provides better wear resistance compared to the conventional cast one. The dominant wear mechanism for the spray-deposited alloy was oxidative mechanism, and that for the cast alloy was delamination mechanism.

Mondal et al. [28] have studied the high stress abrasive wear behavior of aluminium hard particle composites and it has been noted that the abrasive wear rate of alloy reduced considerably due to addition of SiC particle and the wear rate of composite decreases linearly with increase in SiC content. It has been also noted that the wear rate decreases linearly with increase in hardness. This signifies that hardness of the materials play an important role in controlling their wear resistance.

# CHAPTER-4

## EXPERIMENTAL WORK

---

In this chapter all the details about the preparation and characterization of samples has been described. In the present work, the spray forming has been utilized to prepare the samples of composites reinforced with ceramic particulates i.e. zircon sand. The spray forming is used to prepare LM13 base alloy (near eutectic Al-Si alloy) and then reinforcing particulates in the same. The series of reinforcement is selected in such a way to see the effect of particulate size variation and immiscible additive element Sn on the composite performance. The series prepared is

1. LM13 base alloy spray formed
2. LM13-5Sn/zircon sand (63-90 $\mu$ m)
3. LM13-5Sn/ zircon sand (106-125 $\mu$ m)
4. LM13-10Sn/ zircon sand (106-125 $\mu$ m)

A brief description of the raw materials used in the synthesis of composite is presented as below:

### 4.1 Matrix material

LM13 alloy was cut from its ingot size into smaller pieces by an electric power saw in order to feed the crucible properly. Chemical composition of LM13 alloy is given in the Table 4.1.

**Table 4.1** Chemical composition of LM13 alloy

Si	Fe	Cu	Mn	Mg	Zn	Ti	Ni	Pb	Sn	Al
11.8	0.37	1.23	0.41	0.94	0.21	0.025	0.94	0.029	0.01	balance

## 4.2 Reinforcement material

Zircon sand was used as reinforcement material. Particle size of as received zircon sand was in the range between 63-200  $\mu\text{m}$ . The as received reinforcement particle were sieved and required particle size were selected as given in the table 4.2

**Table 4.2** Particle size range of zircon sand

Reinforcement	Particle size range ( $\mu\text{m}$ )
Zircon sand	63-90
Zircon sand	106-125

Chemical composition of the zircon sand used in the present work is given in the table 4.3

**Table 4.3** Chemical composition of zircon sand

Component	ZrO <sub>2</sub>	SiO <sub>2</sub>	TiO <sub>2</sub>	Fe <sub>2</sub> O <sub>3</sub>	Volatiles
Wt.%	65.30	32.80	0.27	0.12	1.51

## 4.3 Process description

The spray deposition system basically consists of a spray assembly to produce spray of fine droplets and an atomization chamber wherein spray atomization takes place in an inert gas atmosphere. The alloy is melted in a graphite crucible placed in an resistance furnace. The molten metal is poured through the crucible into the atomization zone. The atomization zone consists of a convergent-divergent nozzle. In the atomization region, the molten metal stream is disintegrated into spray of droplets by gas jets. The droplets are cooled by the gas stream and accelerated towards a deposition substrate on which they impinge and consolidate to form a coherent deposit. Reinforcement particulates are supplied to the matrix material in the spray cone at some distance from the atomization zone. The reinforcing particles are injected in the spray using injectors under the effect of low pressure inert gas. The particles interact with the liquid droplets in the spray and travel towards the substrate. These are dragged by the droplets or pull

under gravity. This result in co-deposition of particulates with the matrix metal to give rise to a coherent preform of composite material.

#### **4.4 Experimental procedure**

The base alloy used in the present work is LM13 alloy. The alloy was melted in a graphite crucible using an induction furnace. A gas regulator controlled the flow rate of N<sub>2</sub> gas for atomization. The atomization was carried out at a N<sub>2</sub> gas pressure of 100 lb/inch<sup>2</sup>. In our experiment, we are using convergent-divergent nozzle whose diameter is 8mm. Zircon sand having particle size range 63-90μm and 106-125μm were injected through two injectors having 5mm diameter, in the spray closer to the atomization zone of the melt.



**Fig. 4.1:** Spray casting set up.

The spray was subsequently deposited over a copper substrate centered along the spray axis to achieve a circular shape preform of 160mm diameter with a height of 25mm. A nozzle to substrate distance of 30cm was invariably used in all the experimental runs. Several samples were machined from different regions of the spray-deposits for micro-structural examination. The over-spray powder was also collected for further examination.

## 4.5 Materials characterization

### 4.5.1. Optical microscopy

The samples for the micro-structural investigation were prepared following the standard metallographic procedure of grinding and polishing. All the samples were etched in a Keller's reagent. The chemical composition of Keller's reagent is given in the Table 4.6. The micro-structural examination was carried out on Nikon eclipse MA-100 optical microscope.

**Table 4.4** Chemical composition of Keller' reagent

Composition	Dist. Water	HNO <sub>3</sub>	HCl	HF
Volume %	95ml	2.5ml	1.5ml	1ml

### 4.5.2. SEM

The etched samples were seen characterized through SEM (Jeol, JSM-6510 LV, Japan). Micro structural analysis and particle distribution throughout the matrix has been observed in scanning electron microscope.

### 4.5.3. Hardness

The harness test were caring out using digital Rockwell hardness tester (model no. TRSND, fine manufacturing Industries India) with 100kg load and diamond ball as an indenter whose diameter is 1/16 inch on B scale.

#### **4.5.4. XRD**

The X-ray diffraction patterns of the prepared samples were recorded on Panalytical X'pert Pro MPD, Netherland using Cu K $\alpha$  radiation ( $\lambda = 1.54 \text{ \AA}$ ). To know about the phases present in the composite, the composites are characterized by X-ray diffractometry.

#### **4.5.5. Wear**

Dry sliding wear tests were carried out with a pin-on-disc type machine, using specimens in the form of pins with 8mm diameter. The model number of the machine is TR-20 CH 400 Ducom, Bangalore. The wear surfaces were first ground and then polished through diamond paste prior to wear testing. The sliding velocity was fixed at 1.6 m/s. The experiment has been designed with variable loads (2.5kg, 3.5kg and 4.5kg). However the wear characteristics have been noted down at two different temperatures i.e. 50°C and 75°C.

# CHAPTER-5

## RESULTS AND DISCUSSION

This chapter contains the discussion on the results obtained from characterizations done by different techniques on the prepared composites and base LM13 alloy. The detailed study of the results is as follow:

### 5.1 X-ray analysis

Fig. 5.1 shows the XRD pattern of various samples. The collected data were matched with reference data for identification of different phases. The presence of Al, Si, Sn and zircon sand can be confirmed from the XRD plots as shown in Fig.5.1. The reference sources for matching the peaks are Al (ICDD card no. 040787); Si (ICDD card no. 772111); Sn (ICDD card no. 040673) and  $ZrSiO_4$  (ICDD card no. 831382).

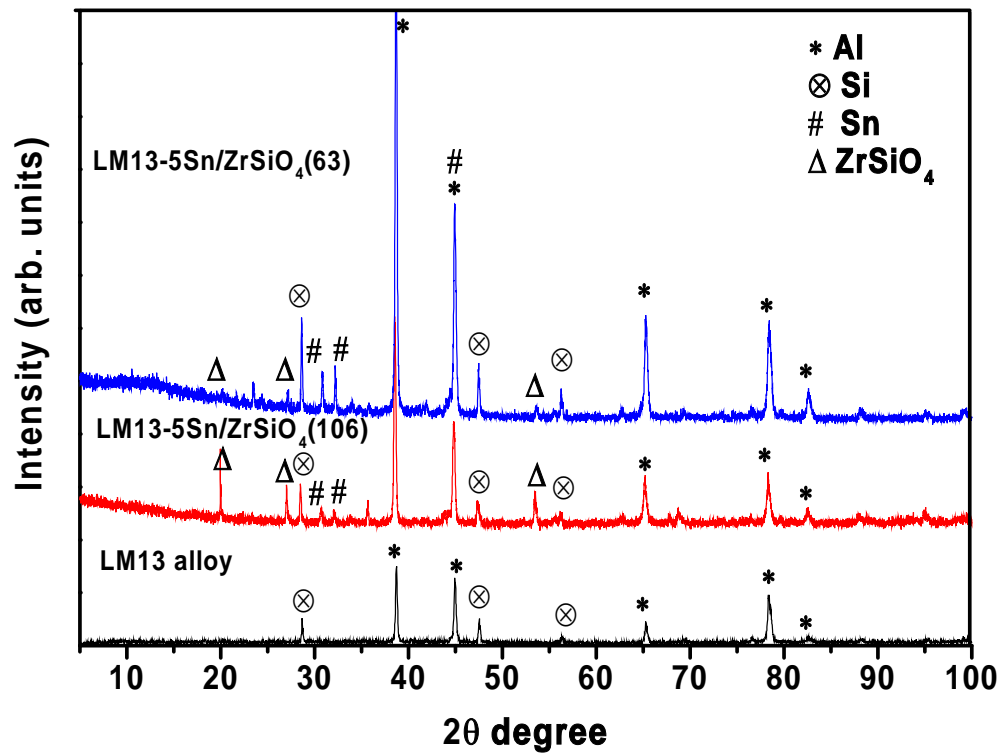
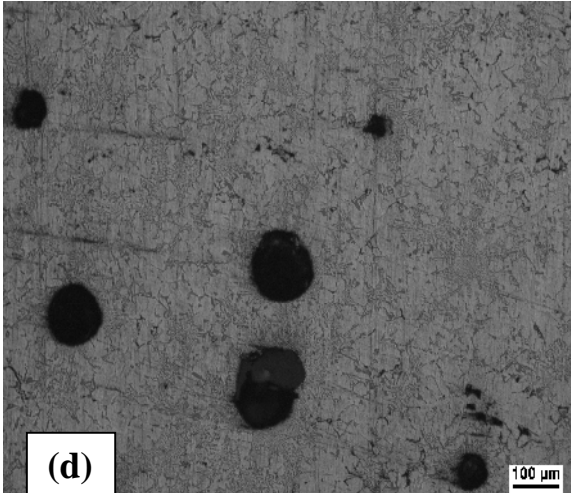
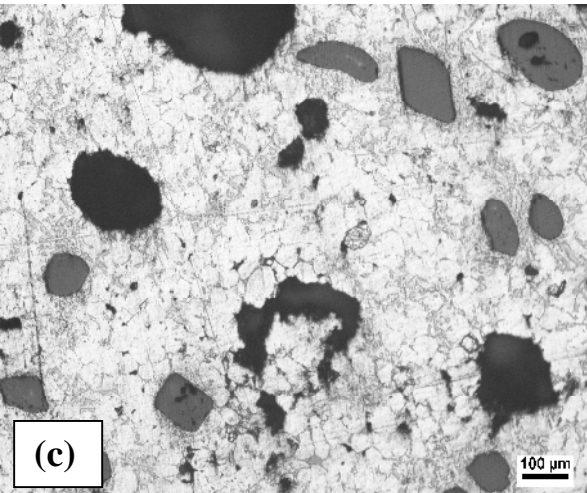
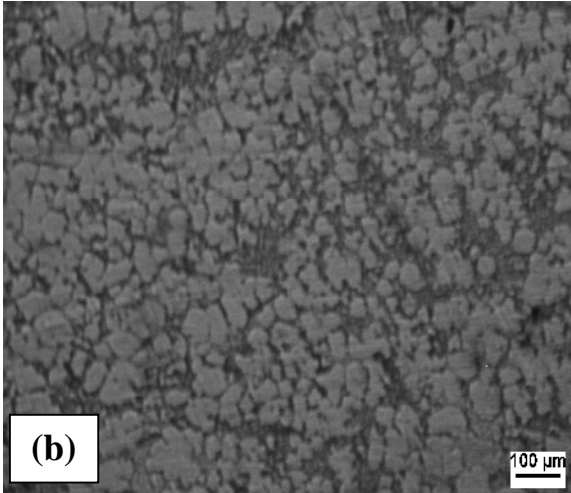
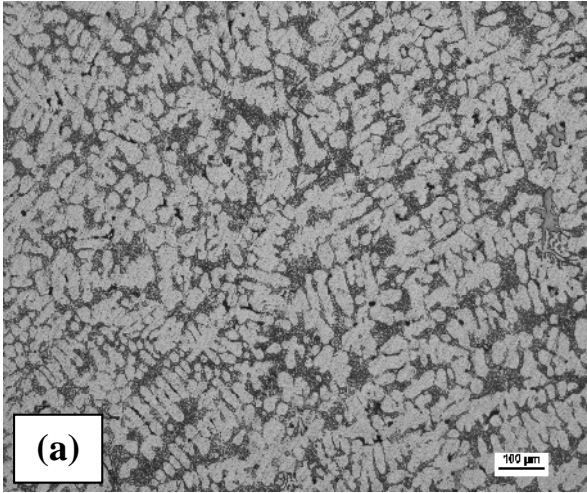
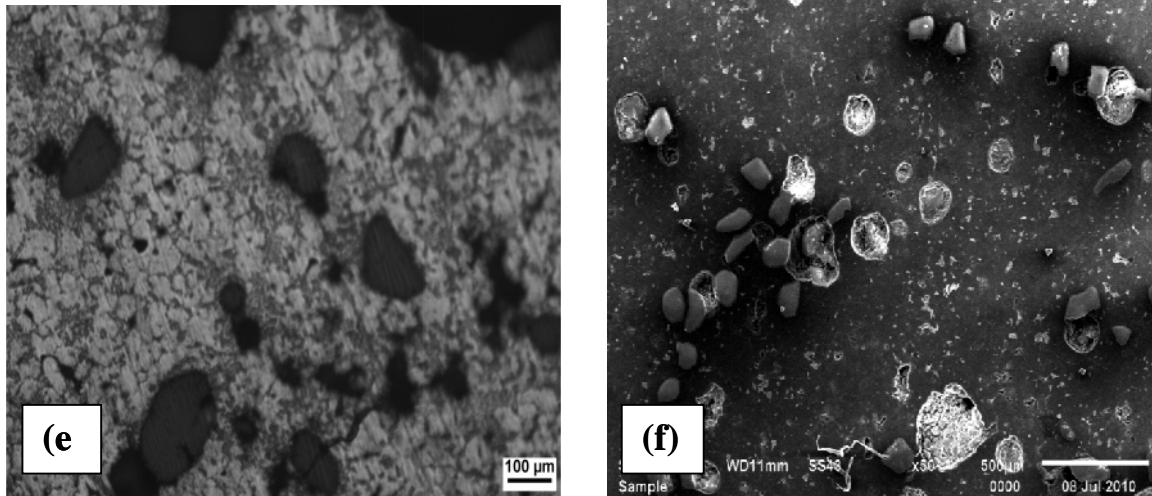


Fig. 5.1 XRD pattern of LM13 alloy and spray formed composites.

5.2 Microstructural analysis





**Fig. 5.2** Microstructure of (a) cast LM13 alloy, (b) spray cast LM13 alloy, (c) LM13-5Sn/zircon sand (63), (d) LM13-5Sn/zircon sand (106), (e) LM13-10Sn/zircon sand (106).

The microstructure of the as cast LM13 alloy and spray formed LM13 alloy is shown in Fig. 5.2 (a,b). An equiaxed grain morphology of the primary  $\alpha$ -phase is distinctly observed in the deposit of spray cast LM13 alloy in contrast to a typical dendritic morphology of the primary phase observed in the cast LM13 alloy which is not desired for better mechanical property. The spray deposited LM13 alloy shows uniform distribution of primary Si phase with a particulate morphology. The white phase as shown in all the microstructure is the  $\alpha$ -phase Al called as matrix phase and dark phase in the microstructure is the eutectic silicon phase. The microstructure of zircon reinforced composite is shown in Fig. 5.2(c, d, e). The particles are uniformly distributed with some amount of porosity in Fig. 5.2(c). In Fig. 5.2(d), particles are embedded along with porosity which can deteriorate the mechanical properties like hardness and wear behaviour. The optical and SEM image of LM13-10Sn/zircon sand are shown in Fig. 5.2(e and f) respectively which shows the distribution of particulate type of morphology in the matrix.

### 5.3 Hardness

Fig. 5.3 shows the Rockwell hardness at B scale of cast LM13 alloy, spray cast LM13 alloy and zircon sand reinforced LM13 alloy with variable particulate size. It has been observed that the hardness of spray formed LM13 alloy is greater than cast LM13 alloy. The higher value of hardness in spray formed alloy is due to the microstructural refinement as shown in Fig. 5.2(b). The fine grain size with equiaxed morphology increases the hardness of the LM13 alloy as processed by spray forming technique.

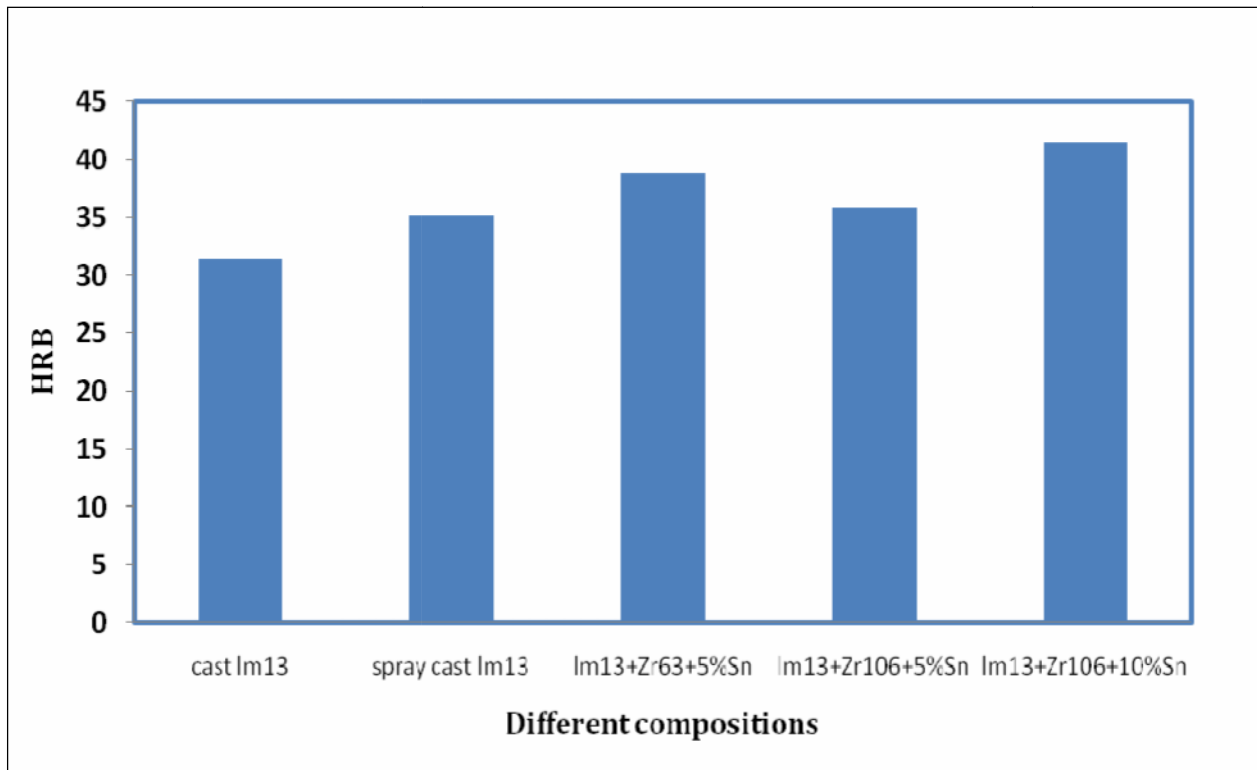


**Fig. 5.3:** Rockwell hardness of different compositions.

The hardness of zircon reinforced composite is more than that of spray cast LM13 alloy. It is also observed that the decrease in particle size from 106-125  $\mu\text{m}$  to 63-90  $\mu\text{m}$  increases the hardness of the composites. The hardness of the composite depends on the hardness of the reinforcement and the matrix. The higher the amount of particle-matrix interface, the more is the hardening due

to hindrance in movement of dislocations. Smaller particle reinforced composite have more particle-matrix interface compared to larger particle reinforced composite for same amount. Hence, the hardness of the composite increases with the decrease in particle size of the reinforcement. Further enhancement of hardness has been obtained with the increase in amount of Sn to 10%.

## **5.4 Wear characteristics**

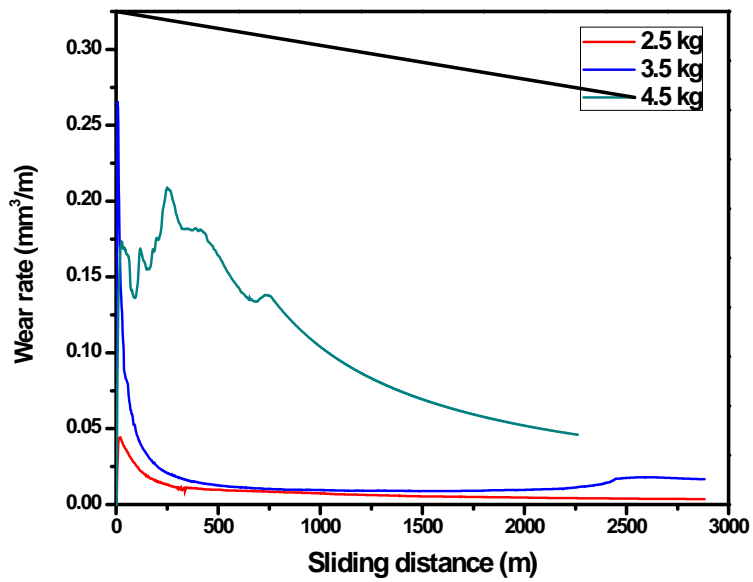
### **5.4.1 Effect of sliding distance**

The wear rate behavior against sliding distance has been recorded at 2.5kg, 3.5 kg and 4.5 kg load for as cast and spray formed LM13 alloy and LM13/zircon sand composite as shown in Fig. 5.4.1(a,b) – 5.4.5(a,b) measured at two different temperatures 50°C and 75°C.

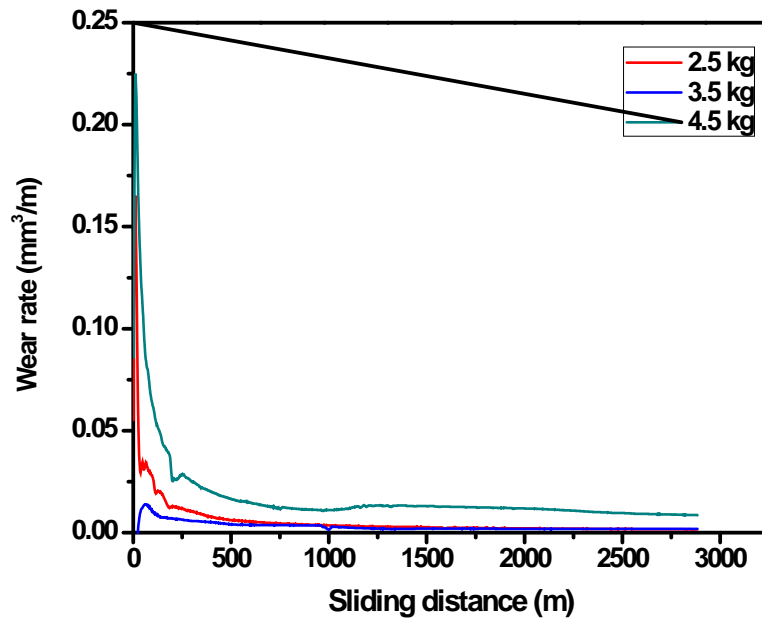
The results shows two different regimes in the trend of wear rate. The curves signify the run in wear rate in initial stage and constant wear rate in the later stage. This behaviour is analogous to the wear rate obtained from respective material at various applied loads. It has been found that initial run in wear is much larger from steady state wear rate. The higher slope up to 500 m gives the information about greater volume loss in initial phase which correspond to the run in wear as already depicted in Fig. 5.4.1-5.4.5. Gupta et al. [29] reported the similar results for dry sliding wear characteristics of 0.13% carbon steels. For both cast and spray formed LM13 alloy (Fig. 5.4.1 and Fig. 5.4.2) a steady state is approachable after 500m sliding distance for all applied loads except higher load of 4.5kg. However, for reinforced composite the stabilized wear is attained at about 300m sliding distance (Fig. 5.4.3-5.4.5). These results are analogous to dry sliding block-on-ring wear test of squeeze cast A390 reinforced with 20% SiC at 45 N and 3.3 m s<sup>-1</sup> observed by Ma et al. [30]. Wear rate was also found to increase in ascending order with applied loads. Similar findings have been also reported by Chaudhury et al. [31] in the Al–2Mg–TiO<sub>2</sub> system for spray and stir cast composites.

Fig. 5.4.3 and Fig. 5.4.4 shows the wear rate at 50° C and 75 °C temperature for zircon sand reinforced LM13 composite of 63-90 µm and 106-125 µm particle size respectively. This has been found that the lower particle size of zircon sand are able to reduce the wear rate more as compare to the bigger size of particulate in the same matrix. On comparing the wear rate at each load it has been found that the wear resistance offered by spray processed composite is higher than base LM13 alloy and reinforced zircon sand composites as shown in Fig. 5.4.3-5.4.5 (a,b).

This shows the good interfacial bonding of zircon sand particle and matrix phase. Moreover, wear rate in LM13-10Sn/zircon sand (106) reinforced composite (Fig.5.4.5) is lower than LM13-5Sn/ zircon sand(106) reinforced composite (Fig.5.4.4). It depicts that on increasing the amount of Sn the wear rate decreased for same particle size zircon sand reinforced composite. Sn is a soft metal and generally used in babbitt alloys as a solid lubricant in plain bearings. The Sn metal solidifies along the grain boundaries of aluminium. This Sn provide an interface between the pin and wheel while sliding. As the pin wears the harder particulate is exposed, with the matrix eroding somewhat to provide a path for lubricant to flow between the rubbing surfaces. It provides an anti-frictional surface to reduce wear. Further, microstructural analysis of the wear surfaces and wear debris is necessary to understand the wear mechanism.

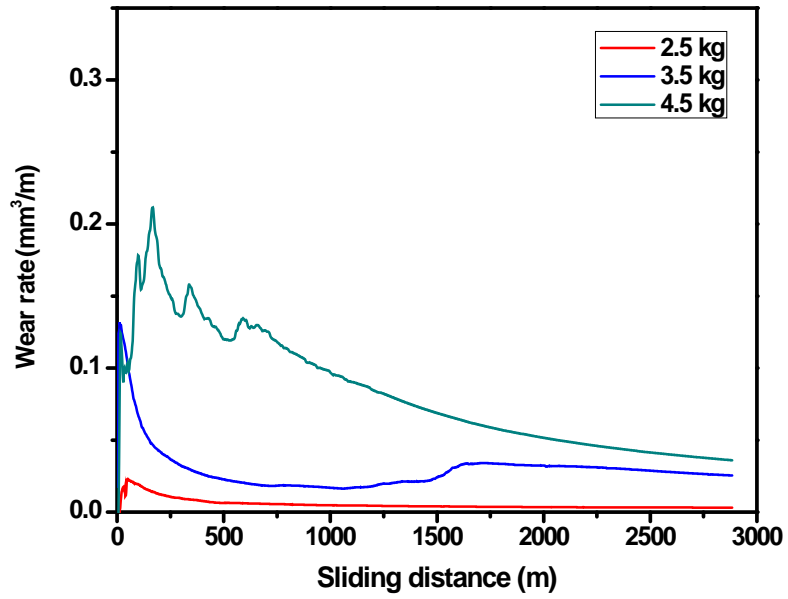


(a)

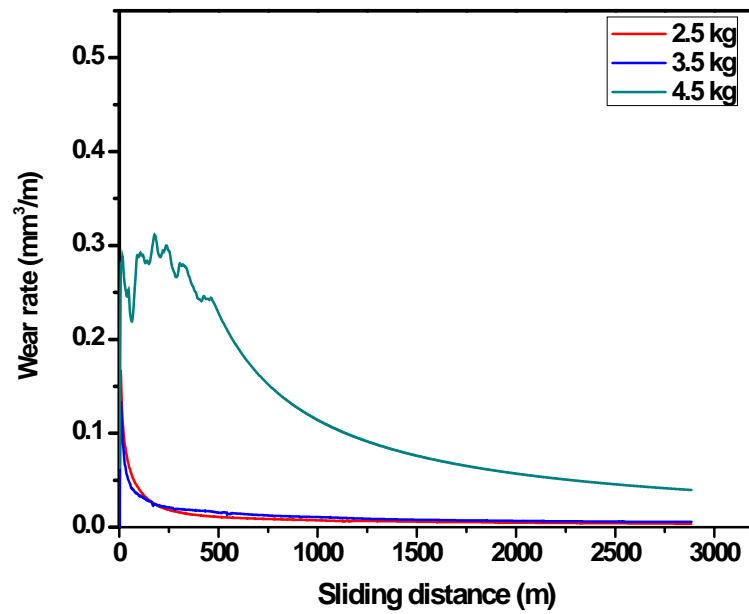


(b)

**Fig. 5.4.1:** Variation of wear rate vs. sliding distance for cast LM13 alloy at (a) 50°C (b) 75°C.



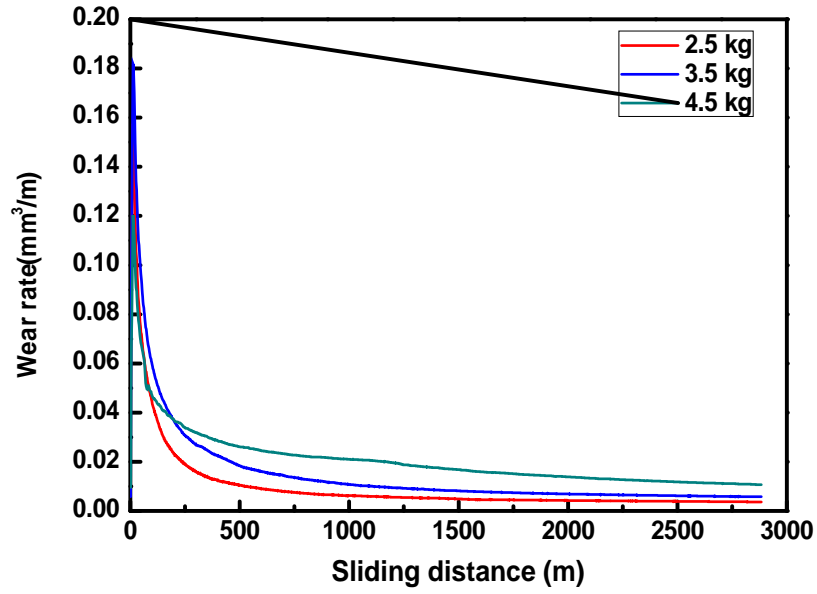
(a)



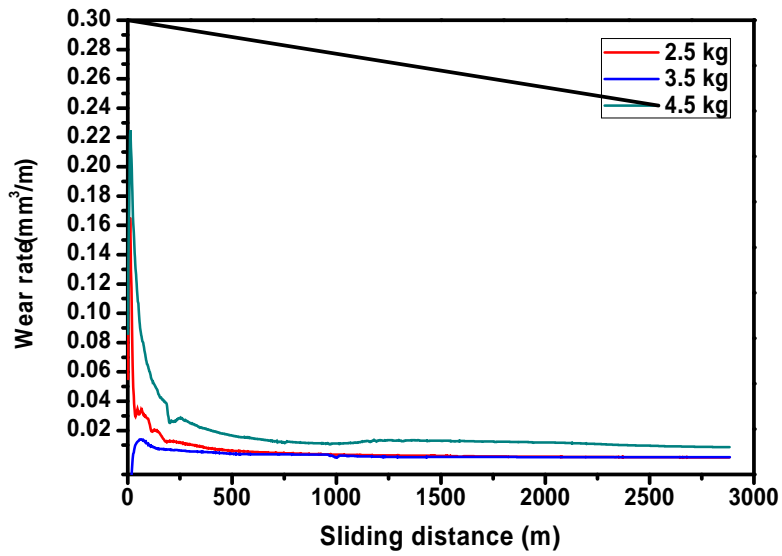
(b)

**Fig. 5.4.2:** Variation of wear rate vs. sliding distance for spray formed LM13 alloy at (a) 50°C

(b) 75°C.

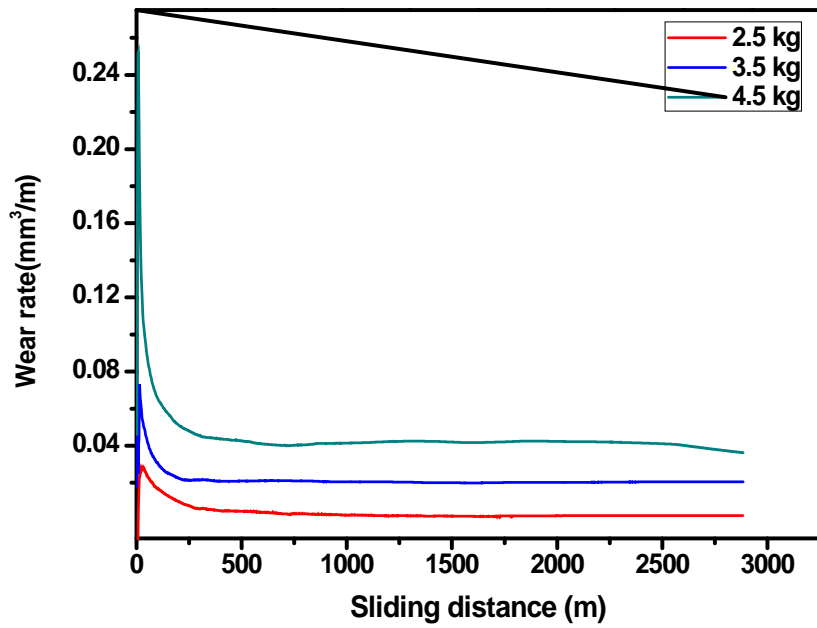


(a)

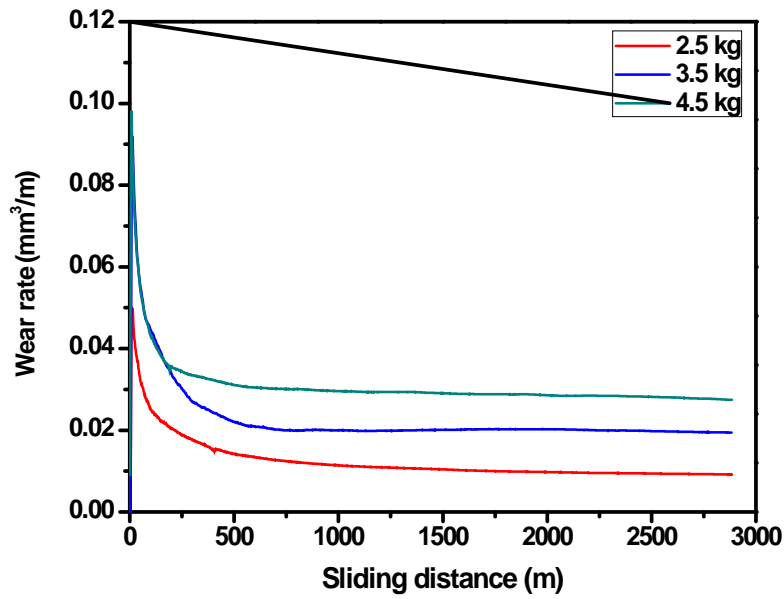


(b)

**Fig. 5.4.3:** Variation of wear rate vs. sliding distance for  $ZrSiO_4(63)$  reinforced LM13-5Sn at (a)  $50^\circ C$  (b)  $75^\circ C$ .

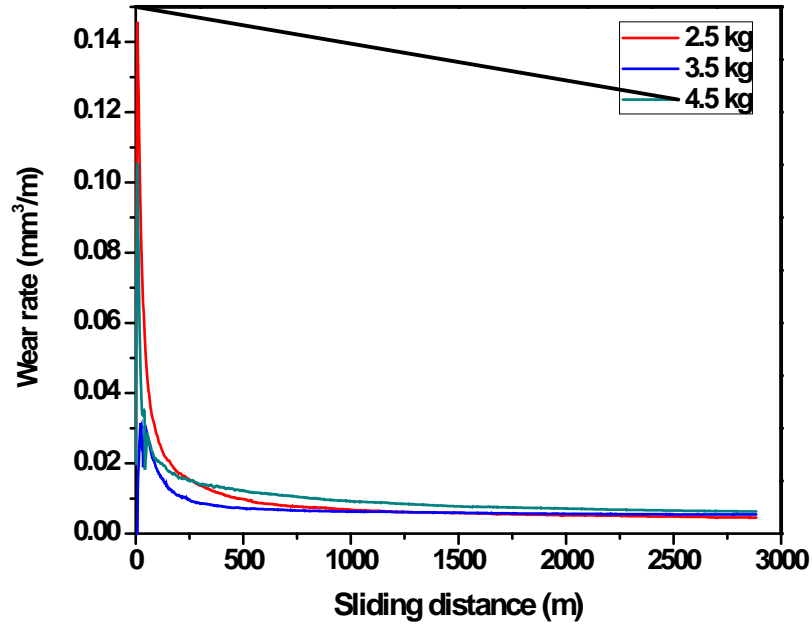


(a)

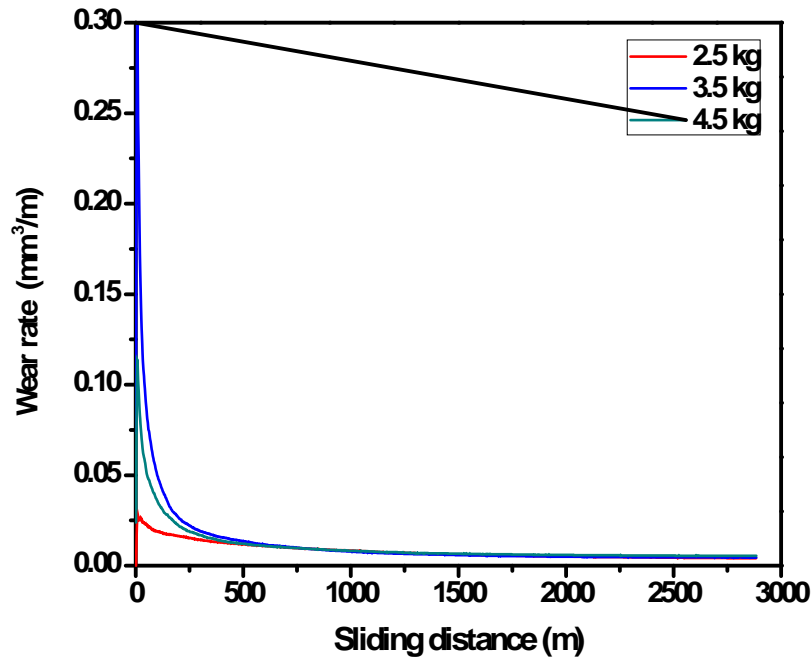


(b)

**Fig. 5.4.4:** Variation of wear rate vs. sliding distance for  $ZrSiO_4(106)$  reinforced LM13-5Sn at (a)  $50^\circ C$  (b)  $75^\circ C$



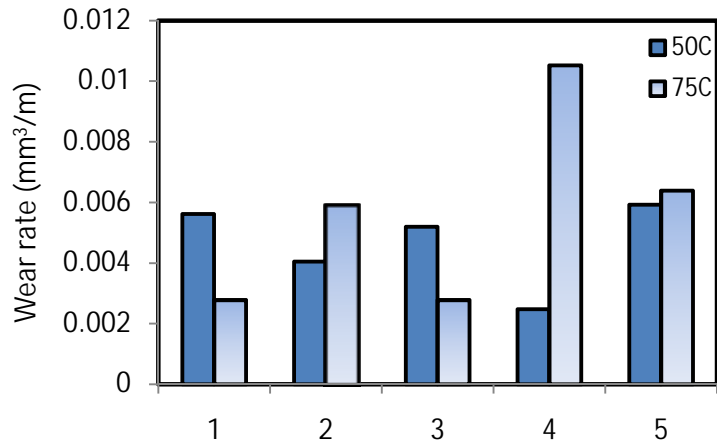
(a)



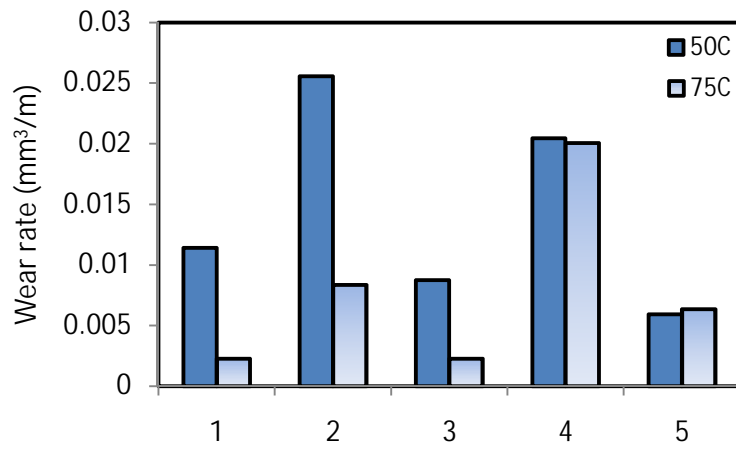
(b)

**Fig 5.4.5** Variation of wear rate vs. sliding distance for ZrSiO<sub>4</sub> (106) reinforced LM13-10Sn at (a) 50°C (b) 75°C.

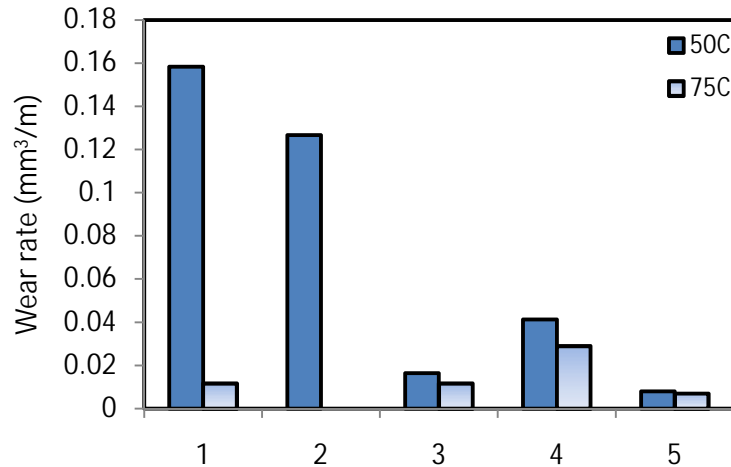
### 5.4.2 Effect of composition on wear rate



(a)



(b)

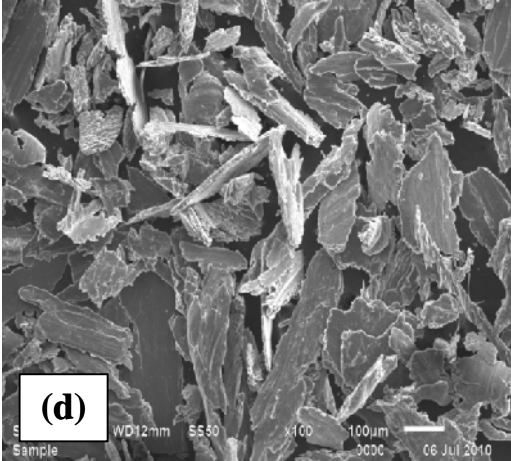
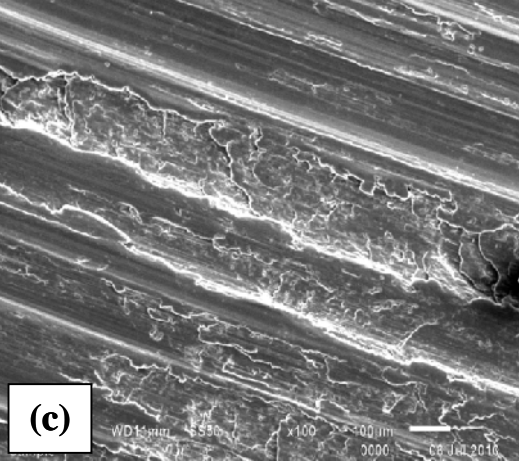
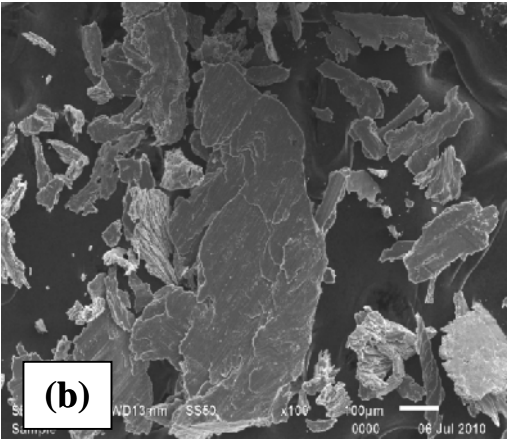
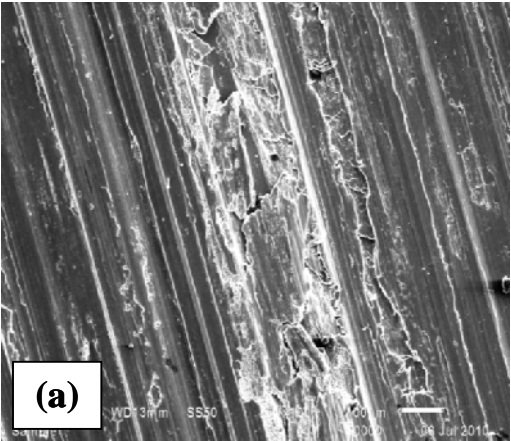


(c)

**Fig. 5.4:** Average wear rate of materials (1-cast LM13; 2-spray formed LM13; 3-LM13-5Sn/zircon sand(106); 4- LM13-5Sn/ zircon sand(63); 5- LM13-10Sn/ zircon sand(106) at 50°C and 75°C for (a)2.5 kg, (b)3.5kg and (c)4.5kg load.

The average wear rate has been calculated for each load after the steady state is approached i.e. after 500m sliding run. The results of average wear rate are shown in the Fig. 5.4 where the averaged wear rate has been plotted against various compositions at both the temperatures 50°C and 75°C. At 50°C, it has been found that for 2.5kg and 4.5kg load spray formed composites are imposing greater resistance to the wear as compared to cast LM13 alloy. However, the data collected at 3.5 kg load is conflicting which might be due to the change in the wear mode in both alloy and composite. At higher temperature 75°C and lower load cast alloy behave well in resisting wear. But at lower load and higher temperature composites are less effecting in resisting wear. From all the five compositions LM13-10Sn/zircon sand(106) has offered the good wear characteristics at higher temperatures due to the higher content of Sn additive in the LM13 alloy which caters lubrication effect. Moreover, at lower load LM13-5Sn/ zircon sand (63) offers greater wear than LM13-5Sn/ zircon sand (106) but at higher load the situation becomes completely reverse. Therefore it is necessary to know the operative wear mechanism for these samples under these alterations. The mechanism of wear can be found with microstructural analysis of the worn pin and collected debris.

**5.5 Analysis of worn pin and debris**



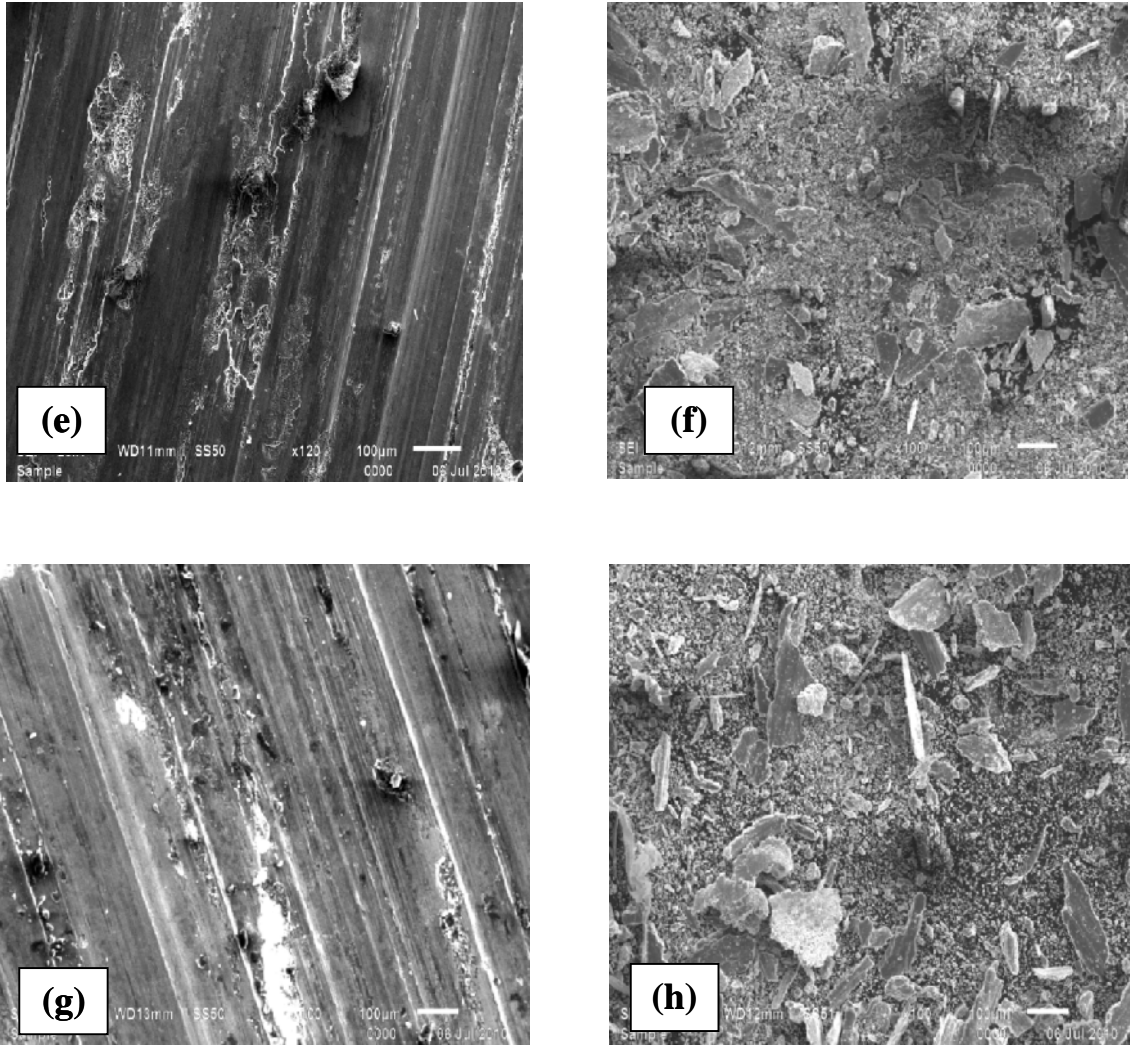


**Fig. 5.5:** At 3.5 kg load SEM images of (a) worn surface of cast LM13 at 75°C, (b) debris of cast LM13 at 75°C, (c) worn surface of spray cast LM13 at 75°C, (d) debris of spray cast LM13 at 75°C, (e) worn surface of LM13-10Sn/zircon sand<sub>106</sub> at 50°C, (f) debris of LM13-10Sn/zircon sand<sub>106</sub> at 50°C, (g) worn surface of LM13-10Sn/zircon sand<sub>106</sub> at 75°C, (h) debris of LM13-10Sn/zircon sand<sub>106</sub> at 75°C.

Fig. 5.5 shows the worn surfaces and debris characterized under SEM to understand the wear mechanism. It has been found that in Fig. 5.5(a,c, e and g) the wear grooves run parallel to the sliding direction. Fig. 5.5(a) shows the microcutting marks along the sliding by which the material has been removed from the surface. Moreover, the crack propagation and debris formation in the chunk amount is clearly visible on the track. A chunk of debris formed from the wear in cast LM13 alloy is shown in Fig. 5.5(b). The worn surface of spray cast LM13 alloy has

shown the repetitive plugging of the material inside the grooves as shown in Fig. 5.5(c). Size of debris is small in spray cast LM13 alloy as compare to cast LM13 alloy as shown in Fig. 5.5(d).

A different surface morphology is observed in the composite material as compare to the cast and spray formed LM13 alloy as shown in Fig 5.5 (e). It is observed that wear grooves are fine with few dimples on the worn surface of the zircon reinforced composite subjected at 50°C as shown in Fig. 5.5(e). The morphology of collected wear debris (Fig. 5.5(f)) of the same shows the oxidative wear mechanism working during sliding. The size of the wear debris is greatly reduced from the spray and cast alloy. At 75°C, the width of the grooves (Fig. 5.5 (g)) and wear debris morphology (Fig. 5.5 (h)) is similar to the worn surface at 50°C except the shining Sn-phase at higher temperature is greater at the surface. It has been found from the worn pin morphology of composite at the surface is shallow as compared to the wear tracks of cast and spray formed LM13 alloy. This indicate that the wear in composite should be less than that from the both alloys. This is again justified from the Fig. 5.4(b) for samples 1, 2 and 5. Moreover, similar morphology at both temperatures is again visible from the average wear calculated for sample 5 in Fig. 5.4(b).

One of the key features observed for plain alloys (both as cast and spray formed) is that the debris show metallic character. The size of these debries are of bigger one and moreover, some of them are twisted also indications that these debries come out as a chunk particle and remain at the track. These are further rolled when trapped beneath the pin during subsequent movement. However, in case of composites a mixed morphology of debries are seen which comprises of long and splat debries alongwith fine one. The twisted features are absent. This variation in debries also indiacte the presence of different mode of wear machanism character in both the cases.

## CHAPTER-6

### CONCLUSION AND FUTURE SCOPE

---

The study of as cast alloy and spray formed zircon sand reinforced LM13 composite led to following conclusions:

1. The composite materials have been successfully prepared with spray forming process.
2. The optical microscopy reveals good zircon particle/matrix bonding with a small amount of porosity along the particles. Also the particles are equally distributed throughout the matrix.
3. The bulk hardness is found to increase on addition of zircon sand particles in LM13 alloy. It has been also observed that the decrease in reinforced particle size increases the hardness of the composites.
4. There is an extensive difference in the morphology of as cast LM13 alloy and spray processed particulate reinforced composite. Despite of dendritic growth of  $\alpha$ -Al grains in ingot cast alloy, equiaxed grains of  $\alpha$ -Al are obtained in spray formed composite.
5. The results indicate that the lower particle size of zircon sand are able to reduce the wear rate more as compare to the bigger size particulates in the same matrix and on increasing the amount of Sn the wear rate decreased for same particle size reinforced composite.
6. It has been found that for 2.5kg and 4.5kg load spray formed composites are imposing greater resistance to the wear as compared to cast LM13 alloy. However, the data collected at 3.5 kg load is conflicting which might be due to the change in the mode of wear in both alloy and composite material.

## **Future scope**

Spray forming offers the potential to reduce costs associated with PM manufacture of Al-Si alloys. Spray formed Al-Si based alloys have been investigated for automotive applications because of attractive combinations of low thermal expansion and greater mechanical properties. The commercial viability of the spray forming process is markedly influenced by the yield and lower cost of usable product i.e. the proportion of the metal atomized which is deposited on the substrate. This in turn is dependent on the design of the equipment, the spray pattern, and the coordinated movements of the substrate. However, there is lot of future scope to improve the material properties by varying the processing parameters of spray conditions. Moreover, a detailed study is required for different size of reinforcing particles. This will enable to have a same cast substance for any structural application.

## REFERENCES

---

- [1] Das S., Das S. and Das K., “Composites science and technology”, vol. **67**, 746-751 (2007).
- [2] Chaudhury S. K. and Panigrahi S. C., “Influence of TiO<sub>2</sub> particles on recrystallization kinetics of Al-2Mg-TiO<sub>2</sub> composites”, J. of materials processing technology, vol. **182**, 540-548 (2006).
- [3] Srivastava V. C. and Ojha S. N., “Microstructure and electrical conductivity of Al-Si composites produced by spray forming process”, Bull. Mater. Sci., vol. **28**, 125-130 (2004).
- [4] Grant P. S. “Spray Forming”, Progress in material science, vol. **39**, 497-545 (1995).
- [5] Spray forming- Wikipedia, the free encyclopedia  
[http://en.wikipedia.org/wiki/Spray\\_forming](http://en.wikipedia.org/wiki/Spray_forming).
- [6] Carter W. T., Benz M. G., Basu A. K., Zabala R. J., Knudsen B. A., Jones R. M., Lippard H. E. and Kennedy R. L., “The CMSF Process: The Spray Forming of Clean Metal”, J. of metals, Vol. **51**, 112-135 (1999).
- [7] Salamci E., “Spray casting”, G.U.Journal of science, Vol. **17**, 155-173 (2004).
- [8] Lavernia E. J., “Spray deposition and atomization”, John wiley and sons, 70-71 (1996).
- [9] Leatham A., “Spray forming: alloys, products & markets”, J. of metals, Vol. **51**, 70-95 (1999).
- [10] Kimirani C. S., Bolfarini C. and Filho W. J. B., “Formation of novel microstructures by spray deposition process”, vol. **403**, 45-50 (2002).
- [11] Raju K., Ojha S. N. and Harsha A. P., “Spray forming of aluminum alloys and its composites: an overview”, J. Mater Sci., vol. **43**, 2509-2521 (2008).

- [12] Srivastava V. C., Mandal R. K., Ojha S. N., “Microstructure and mechanical properties of Al-Si alloys produced by spray forming process”, vol. **68**, 555-558 (2001).
- [13] Satyanarayana. K. G., Ojha S. N., Kumar N. N. and Sastry G. V. S., “Studies on spray casting of Al-alloys and their composites”, Material science and Engineering A, vol. **304**, 627-631 (2001).
- [14] Lavernia E. J., “Synthesis of Discontinuously Reinforced Metal-matrix Composites Using Spray Atomization and Co-injection”, J. Defence Science, vol. **43**, 301-321 (1993).
- [15] Yan S. P., “An aluminum alloy metal matrix discontinuously reinforced with silicon carbide particulates”, J. of material science, vol. **22**, 105-124 (1995).
- [16] Pandey O. P. and Ojha S. N., “Influence of spray atomization and deposition processing on microstructure and mechanical behaviour of an aluminum alloy metal-matrix composite powder”, J. of material science, Vol. **30**, 227-235 (1991).
- [17] Chaudhury S. K., Sivaramkrishnanand S. C., “A new spray forming technique for the preparation of aluminium rutile (TiO<sub>2</sub>) in situ particle composite”, J. of Materials processing Technology, vol. **145**, 334-356 (2004).
- [18] Gupta V., “The microstructure thermal stability, and elevated temperature mechanical behaviour of Al-Ti-SiC metal matrix composites”, J. Defence Science, vol. **55**, 321-345 (1992).
- [19] Santos. H. O., Kuniوشي C. T., Rossi. J. L and Costa. I., “The Corrosion Behaviour of a Hypereutectic Al-Si Alloy Obtained by Spray Forming in Acid, Neutral and Alkaline Solutions”, Materials Science Forum, vol. **530**, 126-131 (2006).
- [20] Jones H., “Formation of microstructure in rapidly solidified materials and its effect on properties”, Materials Science and Engineering A, vol. **137**, 77-85 (1991).
- [21] Kurz W. and Gilgien P., “Selection of microstructures in rapid solidification processing”, Materials Science and Engineering: A, vol. **178**, 171-178 (1994).

- [22] Ferrarini C. F., “Microstructure and mechanical properties of spray deposited hypoeutectic Al–Si alloy”, *Materials Science and Engineering A*, vol. **34**, 577–580 (2004).
- [23] Salamci E., “Mechanical Properties of Spray Cast 7XXX Series Aluminium Alloys”, *J. Eng. Env. Sci.*, vol. **26**. 345 – 352 (2001).
- [24] Wang F., Hu H., Ma Y., Jin Y., “ Effect of Si content on the dry sliding wear properties of spray-deposited Al–Si alloy”, vol. **25**, 163-166 (2003).
- [25] Dasgupta R., “Sliding wear resistance of Al-alloy particulate composites”, *J. Tribology international*, vol. **23**, 132-140 (2009).
- [26] Sursha S., Sridhara B. K., “Effect of addition of graphite particulates on the wear behavior in aluminium-silicon carbide-graphite composites”, vol. **31**, 1804-1812 (2010).
- [27] Wang F., Ma Y., Zhang Z., Xiaohao C. and Jin Y., “A comparison of the sliding wear behavior of a hypereutectic Al-Si alloy prepared by spray-deposition and conventional casting methods”, vol. **256**, 342-345 (2003).
- [28] Mondal D. P. and Das S., “High stress abrasive wear behavior of aluminium hard particle composites”, vol. **39**, 470-478 (2006).
- [29] Gupta V. K., Ray S., Pandey O. P., “Dry sliding wear characteristics of 0.13% carbon steels”, *Materials Science-Poland*, vol. **26**, 617 (2008).
- [30] Ma T., Yamaura H., Koss D. A., Voigt R. C., “Dry sliding wear behavior of cast SiC-reinforced Al MMCs”, *Mater. Sci. Eng. A*, vol. **360**, 116–125 (2003).
- [31] Chaudhary S. K., Singh A. K., Sivaramakrishnan C. S., Panigrahi S. C.,” Wear and friction behavior of spray formed and stir cast Al–2Mg–11TiO<sub>2</sub> composites”, vol. **258**, 759–767 (2005).